

A review of 3D and 4D printing of natural fibre biocomposites

Antoine Le Duigou^{a,*}, David Correa^b, Masahito Ueda^c, Ryosuke Matsuzaki^d, Mickael Castro^a

^a Univ. Bretagne Sud, UMR CNRS 6027, IRDL, F-56100 Lorient, France

^b School of Architecture, University of Waterloo, Cambridge, Ontario, Canada

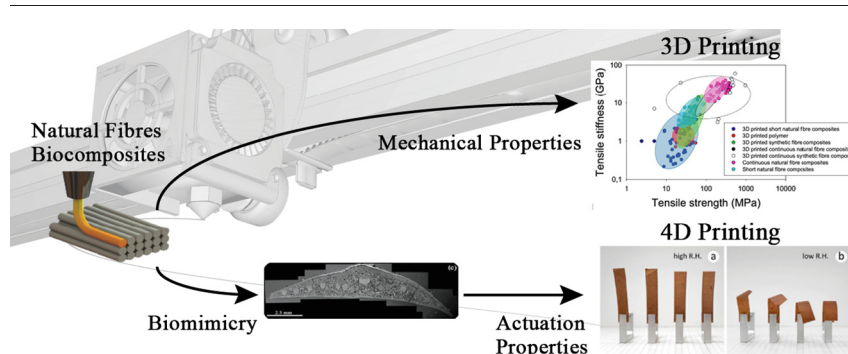
^c Nihon University, 1-8-14 Kanda-surugadai, Chiyoda, 101-8308 Tokyo, Japan

^d Tokyo University of Science, 2641 Yamazaki, Noda, Chiba 278-8510, Japan

HIGHLIGHTS

- The current state of the art on 3D and 4D printing of biocomposites based on natural fibres was achieved.
- The 3D printing data was delivered from the production of the filaments to the tensile properties of the printed biocomposite.
- The 4D printing data of biocomposites were analyzed in terms of actuation characterization.
- The relationship between slicing/printing parameters, microstructure and mechanical or actuation performance was analyzed.
- The future prospects on 3D/4D printing of biocomposites based on natural fibres were discussed.

GRAPHICAL ABSTRACT



ARTICLE INFO

Article history:

Received 24 March 2020

Received in revised form 19 June 2020

Accepted 20 June 2020

Available online 28 June 2020

Keywords:

Natural fibres
Composites
3D printing
4D printing
Hygromorphing

ABSTRACT

To date, the literature has focused on synthetic fibre-reinforced composites, but it has not adequately addressed the unique properties that differentiate natural from synthetic fibres, such as their natural variation in microstructure and composition across species. This review paper proposes a critical overview of the current state of 3D printing of natural fibre-reinforced composites or biocomposites for mechanical purposes, as well as an overview of their role in 4D printing for stimuli-responsive applications. The paper is structured as follows: after the first part recalling the specificities of natural fibres and their associated composites, the two main sections are each divided into two parts presenting an analysis of the available data to provide fundamental understandings and a discussion and outlook for the future.

Natural discontinuous fibre-reinforced polymers exhibit moderate mechanical properties compared to composites manufactured by conventional processes due to specific factors of the 3D printing process, such as high porosity, low fibre content, and a very low fibre-aspect ratio (L/d). Hygromorph BioComposites (HBC) are categorized into a new class of smart materials that could be used for 4D printing of shape-changing mechanisms. Fibre content, fibre orientation control, and fibre continuity are outlined in relation to known challenges in actuation performance.

© 2020 The Authors. Published by Elsevier Ltd. This is an open access article under the CC BY-NC-ND license (<http://creativecommons.org/licenses/by-nc-nd/4.0/>).

* Corresponding author.

E-mail address: antoine.le-duigou@univ-ubs.fr (A. Le Duigou).

Contents

1. Introduction	2
2. Specificities of natural fibre biocomposites for 3D/4D printing	3
3. Natural fibre biocomposites for 3D printing	6
3.1. Filament production	6
3.2. Mechanical properties of natural fibre-based 3D printed biocomposites	8
3.3. Future trends in 3D printing of natural fibre biocomposites	11
4. Natural fibre biocomposites for 4D printing	14
4.1. Principle.	14
4.2. Actuation properties of natural fibre-based 4D printed biocomposites	14
4.3. Future trends in 4D printing of natural fibre biocomposites	18
4.3.1. At the material level	18
4.3.2. At the structural level.	18
5. Conclusion	19
CRedit authorship contribution statement	22
References.	22

1. Introduction

Additive manufacturing has been extensively investigated over the past decade due to its disruptive potential in the design of advanced materials and structures. Among the various additive manufacturing techniques, Fused Filament Fabrication (FFF) 3D printing is one of the most applied techniques to polymers and composites in the literature. The FFF method involves the layer-by-layer deposition of viscous thermoplastic material through a heated nozzle onto the platform or over previously printed layers. The advantages of FFF include shortening the design-manufacturing cycle [1], minimizing the cost for low production runs [2], reducing the production waste [3], being able to build intricate geometries [4], being able to tailor microstructure and properties in each layer [5], and providing high value to research applications [6]. Originally targeting prototyping applications, the development of FFF has gradually moved towards mechanical performance controlled by slicing and printing parameters. Slicing parameters include the raster angle (in-plane angle), the layer height, the interfilament distance, nozzle diameter, the filling pattern (e.g. honeycomb, hexagonal, triangular), the filament orientation, and the build orientation (out-of-plane) [4]. Nozzle geometry, printing speed, printing trajectory, nozzle temperature, bed temperature, and calibration are categorized as printing parameters [4].

The development of fibre-reinforced composites using FFF has enhanced the mechanical properties of 3D printed polymeric parts [7]. However, major work is still required to enable the 3D printed parts to meet the structural application specifications. The main obstacles for printed composites are inherent extrusion-induced defects, such as porosity, which are caused by poor interfacial bonding between the fibres and the polymer [8] and between the printed beads or the printed layers [9]. It is therefore important to distinguish between the properties of the materials and the properties of the printed part [10]. In addition, reinforcing fibres, mainly glass and carbon, influence the printability of composites due to their orientation, geometry, and content [7,11]. Numerous review articles have been published, describing the advantages and disadvantages of 3D printing of composite materials with synthetic fibres, such as the limited mechanical properties, the narrow range of materials available, and their poor surface finish [2,11,12].

Natural fibres and especially bast fibres are used as composite reinforcement to substitute for glass fibres because of their mechanical [13], acoustic [14], or even morphing properties [15] in combination with their low density, reduced environmental footprint, and alternative end-of-life management [16]. However, their application as composite reinforcement cannot be conducted in the same way as their synthetic counterparts. Specific knowledge of their microstructure and

composition-related properties, which vary from one type of natural fibre to another, is required to select them correctly [13]. In addition, it is necessary to take into account their sensitivity to heat and humidity, complex polysaccharidic composition, inherent defects, and natural variability to achieve high performance [17]. Today, most processing routes can be applied to these natural fibre biocomposites with a thermoplastic matrix including extrusion, injection moulding, thermoforming, film stacking, and vacuum bag moulding [16,18,19]. Although biocomposites based on natural fibres were proposed in 1937 (i.e. Gordon aerolite [20]), their development is relatively recent in contrast to their synthetic counterparts. The use of natural fibres has encountered challenges related to a lack of preform availability, technical processing knowledge, lifespan information, and limited understanding of their mechanical behaviour. Recently, additive manufacturing has emerged as an ideal opportunity for biocomposites to fill the gap with synthetics and begin to bring biocomposites to a similar technological maturity. Thus, natural fibres are steadily gaining interest as fillers or composite reinforcements for FFF applications. However, most review articles on 3D printing deal with synthetic composites [2,4,5,11] and do not mention the current trend of research on biocomposites and their unique characteristics. A complete state-of-the-art review of the work carried out to date that also highlights recent trends on 3D printed biocomposites is thus justified.

Starting in 2013, 4D printing is a relatively recent trend to develop 3D printed structures that can change their shape or properties over time [21–23]. 4D printing research aims to achieve a predictable and predefined time-dependent change in functionality (shape, property, self-assembly, or self-repair) that the 3D printed structure undergoes when in contact with an external stimulus (e.g. temperature, ultraviolet light, humidity, electric and magnetic field) [21]. 4D printing involves the development of the raw printing materials and the design of the mechanism and multi-layer architecture of the printed structures that directly incorporate a pre-programmed transformation [24]. A wide range of materials and printing methods are being developed for this purpose, such as Shape Memory Polymer (SMP), Electro-Active Polymer (EAP), and Hygromorph Composites (moisture-induced morphing). The latter can be based on hydrogel [25] or natural fibre biocomposites [15]. The moisture-induced anisotropic swelling of natural fibres has been used as a driver of actuation in the development of hygromorph biocomposites via 3D printing [8,15,26–30]. However, existing review articles on 4D printing provide a very general overview of these smart materials, and offer very limited specificity on the distinctive characteristics of hygromorph biocomposites [3,24,31–34].

The aim of this article is to propose an exhaustive and comprehensive literature review of natural fibre biocomposites manufactured by

3D printing (FFF) and 4D printing with mechanical and actuation features respectively. It should be noted that man-made cellulose and nanocrystalline cellulose are excluded from the scope of the work presented.

First, a general description of natural fibres and their specificities (e.g. microstructure, composition) is given to better understand the challenges for 3D and 4D printing of natural fibre biocomposites. Next, the present review article focuses on the 3D printing of biocomposites from filament production to the current state of their mechanical properties, including a description of the challenges, limitations, and future trends of the process. Finally, the application of natural fibre biocomposites to 4D printing for shape-changing features is reviewed. This includes an overview of 4D printing principles applied to hygromorph biocomposites, their actuation performance, and the future prospects at different levels, from the material to the architected structure (metamaterial).

2. Specificities of natural fibre biocomposites for 3D/4D printing

The properties of 3D and 4D printed composite materials are affected by the type of fibres used, their stiffness, strength, and capacity for interfacial bonding with the polymer matrix. In an ideal scenario, the microstructure of the composite material would be homogeneous, with well-distributed fibres with a high aspect ratio (length/diameter), and the interfacial surface would be maximized to ensure load transfer. To meet this goal, defects or porosity in the matrix and interfacial area should be reduced as much as possible. However, for natural fibres, the mechanical properties (stiffness and strength) are anisotropic and depend on their hierarchical microstructure (Fig. 1a) and their biochemical composition (cellulose, hemicelluloses, pectins, lignin, and water - Table 1). Table 1 indicates the tensile properties, biochemical composition, and microstructure of various natural fibres, features that are needed for the analysis presented in the two sections dedicated to 3D and 4D printing. The relationship between their microstructure, composition, and properties is typical of naturally optimized biological materials. For example, the bast fibres that provide stability to the plant (e.g. hemp, flax) have greater stiffness and strength than fruit fibres dedicated to energy dissipation such as coir fibres [35]. Their secondary cell-wall controls the overall hygro-mechanical properties of the natural fibres owing to the angle of the cellulose microfibrils (MFA) [36,37], the interactions between the components, and their overall composition.

The multi-scale microstructure of natural fibres and their internal interactions between components and cell walls also involve complex non-linear tensile behaviour [41,42]. Unidirectional natural fibre composites also exhibit this non-linear behaviour [43], which makes it

difficult to assess their stiffness. Shah et al. [43] recommend evaluating the tensile modulus in a range of deformations from 0.05 to 0.1% and even more conservatively, i.e., after 0.4% deformation when the stiffness of the composite variation is low. Selecting the right natural fibres according to the part specification (e.g. stiffness, toughness) is the first step in developing a high-performance material for 3D printing.

Next, stress transfer at the interface needs to be considered, as the composite properties depend on fibre length, diameter, tensile properties, and the interfacial shear strength. The surface properties of natural fibres, which control the interfacial shear strength, are more complex than their synthetic counterparts, as can be observed in glass or carbon fibres. For instance, natural fibres are often assembled into a bundle of single fibres that is held together by a pectic cement called middle lamellae (Fig. 1c: diameter of bundle $\approx 200\text{--}400\ \mu\text{m}$ and diameter of single fibre $\approx 20\ \mu\text{m}$). This bundling is the result of the original material architecture of the plant. The scale of the fibre bundle is generally referred to as “technical fibres” in the literature. Retting is an important step for fibre production that involves a natural enzymatic degradation of the middle lamellae in order to facilitate the extraction of the fibres [44]. The retting process also influences the surface roughness of the fibres (Fig. 2a, b and c) and the overall splitting state of the bundles, such as the aspect ratio (reinforcement length to diameter ratio) [45] within the composite.

Scaling a single fibre is achieved after splitting the bundle during retting and mechanical processing (e.g. extrusion, injection [46] and see Fig. 3a), which means that residues of middle lamellae could be deposited on the surface of the fibre and radically change the composition of the surface of the fibre (Fig. 2b and c) [47]. Unlike hemp fibres, the roughness of flax fibres, mainly composed of low molecular weight pectins, does not participate in load transfer and appears as a potential surface defect [39]. Cleaning the fibres with water has been shown to be an effective means of removing low weight pectin and improving practical adhesion with the PolyLactic Acid (PLA) matrix [39]. The fibre surface modification has been extensively examined in the literature, and chemical treatments are often proposed. However, the appropriate stage at which the surface of the fibres is modified should be considered. For example, if the treatments are applied to fibre bundles, it is clear that the efficiency of the treatment will be limited, especially if bundle splitting occurs during high shear rate processing [48] (e.g. extrusion that occurs prior to 3D printing) (Fig. 3a).

In addition, unlike conventional fibre-reinforced polymer composites (e.g. glass or carbon fibre-reinforced polymer), natural fibre composites have multiple hierarchical interfaces, ranging from cell wall components (Fig. 1a), cell wall layers (Fig. 1a), and fibre/matrix (Fig. 1b), to fibre/fibre interfaces (Fig. 1c). Thus, cell-wall peeling occurs during loading of the composite [49]. This mechanism, particularly in

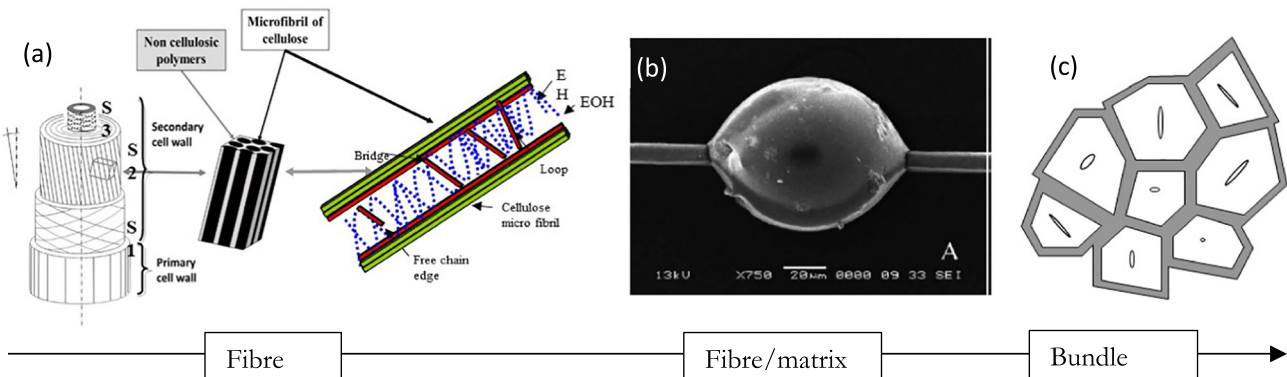
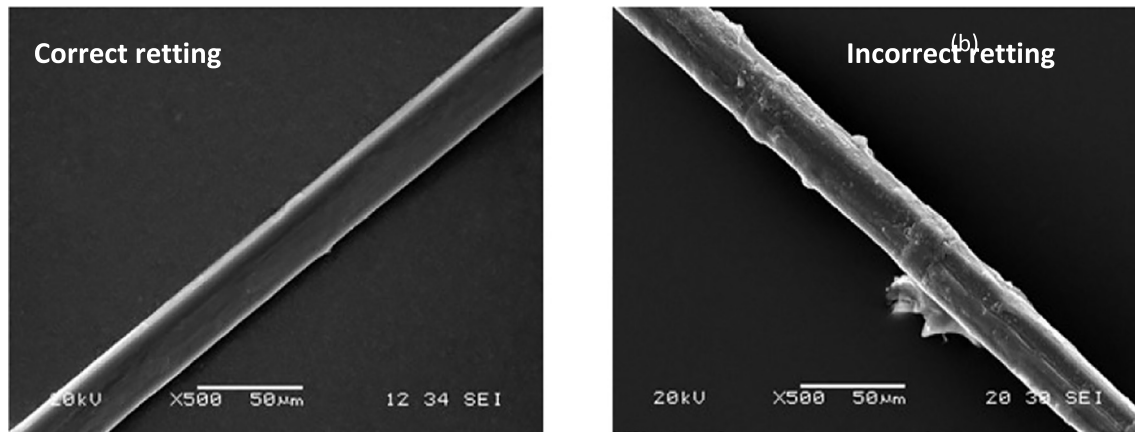


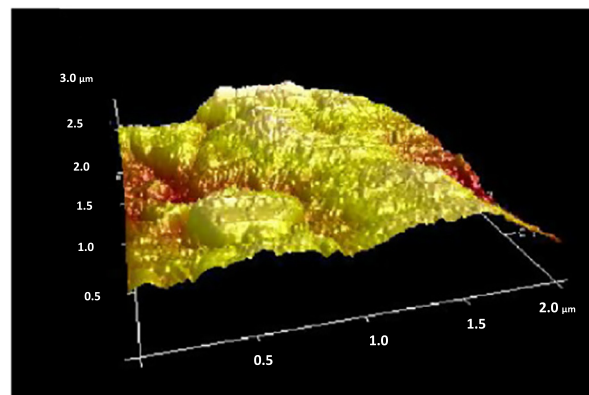
Fig. 1. Description of the different scales required to analyse the natural fibre composites' (a) internal fibre cell-wall interface, (b) fibre/matrix interface, and (c) fibre/fibre interface within the bundles. Adapted from [38–40] with permission from Elsevier.

Table 1
Mechanical characteristics (Tensile modulus and Stress at break) and biochemical composition (Cellulose, Hemicelluloses, Lignin, Pectins content, and microfibrillar angle (MFA)) of various natural fibres used in 3D and 4D printing.

Fibres	E (GPa)	σ (MPa)	Cellulose [%]	Hemicelluloses [%]	Lignin [%]	Pectins [%]	MFA (°)	Ref.
Flax	46–85	600–2000	64–85	11–17	2–3	1.8–2.0	10	[59,60]
Jute	24.7–26.5	393–773	61–75	13.6–20.4	12–13	0.6 ± 0.6	7–12	[35,60–64]
Kenaf	11–60	223–930	45–57	21.5	8–13	3–5	7–12	[29,32,61,[65,66],67]
Coir	3.44–4.16	120–304	32–46	0.15–0.3	40–45	3–4	30–49	[16,35,60,61]
Cotton	3.5–8	287–597	82–99	4	0.75	6	30–40	[68,69]
Wood	15.4–27.5	553–1500	38–45	19–39	22–34	0.4–5	5–45	[13,70]
Bamboo	10–40	340–510	34.5–50	20.5	26	<1	2–10	[68]
Harakeke	14–33	440–990						[19]
Hemp	14.4–44.5	270–889	55–90	4–16	2–5	0.8–8	6.2–11.2	[71–73]



(a)



(b)

Fig. 2. (a) SEM micrograph of single flax fibre surface with correct (left) and incorrect (right) retting. Correct retting leads to a homogeneous smooth surface whereas incorrect retting induces low adherent polysaccharidic residues (b) AFM image of a flax fibre surface with incorrect retting producing a rough surface. Adapted from [39] with permission from Elsevier.

evidence in the micromechanical tests (Fig. 3b), is also observed at the laminate level [48,49]. Its effect on stress transfer is not yet clearly understood but suggests that even if a fibre/matrix interface is chemically or physically optimized, the internal interfaces between cell walls may ultimately be the weakest link.

It can be assumed that the surface of a natural fibre corresponds to its outer layer, i.e. the primary cell wall (Fig. 1a). For a single flax fibre [50–52], the primary cell wall with thickness ranging from 200 to 500 nm is heterogeneously composed of low-crystallized cellulose, hemicelluloses, and pectin. Although it is one of the most biochemically

described fibres in the literature, the exact distribution and quantity in this cell wall and thus the exact surface composition and interactions with the matrix are still unknown. Only the total biochemical composition is currently known (Table 1).

The initial natural fibre bundle length introduced in short fibre biocomposites manufactured by extrusion, injection, or compression moulding varies from 0.1 to several mm [53], but the process drastically affects the reinforcement geometry. For example, one extrusion reduces the length of flax bundles within a PLA matrix from 4 ± 0.6 to 2.3 ± 1.2 mm and the diameter from 182 ± 76 to 133 ± 60 µm [54]. This

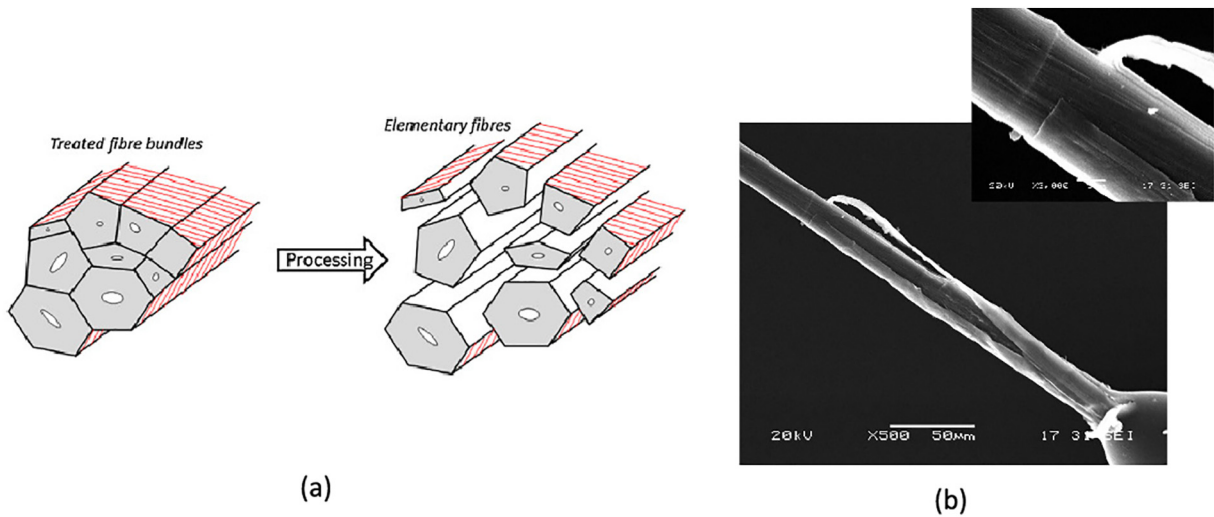


Fig. 3. (a) Example of fibre bundle division into single fibres during processing, highlighting the reduction in the effectiveness of surface treatments [48], (b) Detail of a flax cell wall peeling during microbond testing [39], which indicates that the weakest interface may be the cell wall interface compared to the fibre/matrix interface. With permission from Elsevier.

leads to variable length, diameter, and aspect ratio (L/d) that affect the formation of interfacial porosity [55], the load transfer, and the corresponding mechanical properties [56]. Above a critical fibre length proposed by Kelly-Tyson [57], fibres act as reinforcement and efficient load transfer at the fibre/matrix interface. Below this critical fibre length, fibres are debonded, and the load cannot be transferred properly to the fibres. These geometrical parameters are significant for 3D printing as they also influence the processability of the material [58].

3D printing via FFF is carried out with thermoplastic polymers. The fabrication process requires a thermal cycle of heating in order to reach the melting temperature of the polymer, followed by extrusion and subsequent cooling. Each of these processes directly influences the polymer microstructure and the physical properties of the printed component. Most current polymers or biopolymers that are used with natural fibres are amorphous or semi-crystalline polymers. For example, PLA [74–76], Acrylonitrile butadiene styrene (ABS) [74,77], Polyhydroxyalkanoates (PHA) /PLA blend [29], recycled Polypropylene (rPP) [78], biobased Polyethylene (bioPe) [79], Polycaprolactone (PCL) [80], and thermoplastic Polyurethane (TPU) are used and require a temperature higher than 200 °C to be printed: 210–230 °C for PLA, 210 °C for bioPE, 230–275 °C for ABS, 210 °C for PLA/PHA, 230 °C for rPP, 120 °C for PCL, and 190 °C for TPU [81].

Despite the reinforcing effect of natural fibres, their addition could disrupt the printing process as their polysaccharide components are very sensitive to temperature and moisture. High temperatures (above 150 °C) and long exposure time (above a few minutes) can have a dramatic effect on the mechanical properties of natural fibres. Reduction in their longitudinal and transverse modulus as well as their longitudinal strength [82,83] can occur due to the thermal

decomposition of polysaccharides, evaporation of moisture, and differential shrinkage within the cell wall. Yang et al. [84] have demonstrated that increasing the printing temperature for PLA/wood from 200 to 230 °C reduces the tensile strength by 10% and modulus by 5%, flexural strength by 7% and modulus by 20%. However, due to the printing speed (15–30 mm/s [29,79,84]), the short printing distance, and the cooling temperature control (bed temperature, convection depending on a printing chamber), a high temperature exposure is usually short (i.e. a few seconds).

The manufacturing temperature also has an effect on the properties of natural fibres, their surface quality, and the resulting fibre/matrix interface. For example, a drying of 14 h at 105 °C reduces the interfacial bond strength of flax fibre with PLA by 20% [39] due to embrittlement of the internal interfaces and changes in surface wettability due to the surface migration of low molecular weight components and the reorientation of the surface molecules [85,86].

Moreover, significant residual stresses accumulate as a result of the layer-by-layer process, the in-plane and out-of-plane temperature gradient, the difference in the thermal expansion coefficient between each component (matrix and fibre), the difference in thermal expansion between the plies, and the inhomogeneous cooling or crystallization temperature field [87,88]. Their magnitude depends on the printing speed, the printing angle, and the type of material [89]. Stoof et al. [78] have shown that the addition of an increasing natural fibre content in the rPP matrix reduces its shrinkage to 84% for a sample loaded with 30% of hemp fibre (Fig. 4).

Xiao et al. [90] confirm this observation of Hemp hurds/PLA biocomposites. In contrast to conventional synthetic fibres (glass or carbon), natural fibres such as flax have a high anisotropic Coefficient of



Fig. 4. Pure rPP and 30% hemp/rPP made with 3D printing. Their curvature enables the evaluation of the residual stress and shows the role of hemp fibres to reduce thermal stresses. Adapted from [78] with permission from Elsevier.

Thermal Expansion (CTE), closer to that of conventional polymers (e.g. Polypropylene), which reduces the overall residual thermal strains [91].

However, natural fibres and flax have a very high Coefficient of Hygroscopic Expansion (CHE) due to their sensitivity to moisture and their microstructure (low MFA value) [36]. Therefore, during a heat cycle, flax fibres shrink mainly due to the evaporation of water rather than expand thermally; then, the molten polymer matrix fills all the interstices of the biocomposite (see the black dotted line that expresses the difference of position between initial and dry state in Fig. 5). The magnitude of hygroscopic shrinkage is higher than the thermal expansion of the fibre or polymer (Table 2).

During the cooling stage, the fibres and matrix shrink to different degrees, depending on their coefficient of thermal expansion. Thermal and hygroscopic stresses are generated at the fibre/matrix interface. When stored at 50% RH, flax fibres swell more than the matrix. A hygroscopic stress is produced (Fig. 5). Therefore, the change in humidity during processing as in during storage causes the sample to curve, which is detrimental to mechanical applications. However, this shape transformation has opened up new design windows for 4D printing where moisture is used to trigger actuation (see Section 4) [29].

3. Natural fibre biocomposites for 3D printing

3.1. Filament production

In composite materials, the manufacturing stages of semi-finished products influence the performance characteristics by inducing defects (e.g. porosity, misalignments), mechanical or hygro-thermal degradation, and residual stresses. Filaments are seen as semi-finished products. For the FFF, the filament is produced by a common extrusion process where fibres and polymer are blended together. Further work on natural fibre biocomposite extrusion can be found elsewhere [46,53,95]. Currently, much work is focused on extrusion parameters to produce filaments with hemp fibres [78,96–98], hemp hurds [90], bamboo fibres and powder [99–101], flax fibres [99], bagasse fibres [102,103], cork powder [10,104], cocoa shell [80], coconut fibres [105], cotton fibres [106], wood fibres [74,107], wood pulp [79,108], wood flour [102,109,110], Harakeke fibres [96–98], and waste macadamia nut shell [111]. Even though these can all be considered natural fibres, their composition, microstructure, and tensile properties are highly variable (see Table 1), which leads to a variety of potential functionality

ranging from mechanical reinforcement and acoustical dampening to shape changing.

Although most of the existing data on composite fibre filaments for FFF come from suppliers and data sheets, a growing number of research papers are currently dedicated to customized production of filaments for 3D printing. This has prompted a general shift of 3D printing from a technological to a scientific paradigm, leading to deeper insights into the properties related to the microstructure of the composite fibre filaments. The fraction of natural fibre within the filaments has a direct effect on their surface roughness. An increase in fibre content leads to a rougher filament with visible clustered fibres on the surface (Fig. 6 [80]).

The increase in fibre content also leads to higher porosity [74,79]. For example, the porosity content is between 27.1% and 47% for a wood fibre content varying from 10% to 20% by weight in a BioPE matrix [79].

The chemical treatments of the fibres and the selection of polymers of different viscosities could significantly reduce the porosity content and thickness variations of the filaments [79]. Filgueira et al. [79] have proposed a subsequent extrusion to reduce porosity, fibre agglomeration (fibre size), and roughness due to an improvement of the compounding process (Fig. 7) and reduced fibre geometry. Furthermore, several papers on the recycling ability of natural fibre composites have shown that an increasing number of extrusions were correlated to a reduction of natural fibre length, fibre bundle division, and better homogenization of the blend [112,113].

Depuydt et al. [99] have produced filaments with low porosity (around 0%). They have shown that the application of vacuum at the end of the compounding process (i.e. at the end of the PLA/Flax or PLA/Bamboo metering zone) lowers the porosity content to the limit of measurement (below 2 μm). In addition, drying in an air dryer also results in a reduction in porosity.

The extrusion process during filament production influences the microstructure of the material and thus the properties of the 3D printed part. For instance, a skin/core effect has been observed [99] in some samples with a relatively high fibre aspect ratio, while dust-like bamboo or curved flax fibre counterparts exhibit a random 2D orientation (Fig. 8).

Fibre length, diameter, and aspect ratio (Length/diameter) are also key parameters that control the performance of composite filaments. To produce filaments with a diameter between 1.75 and 3 mm, natural fibres are commonly used with a very low length/diameter (L/d) ratio

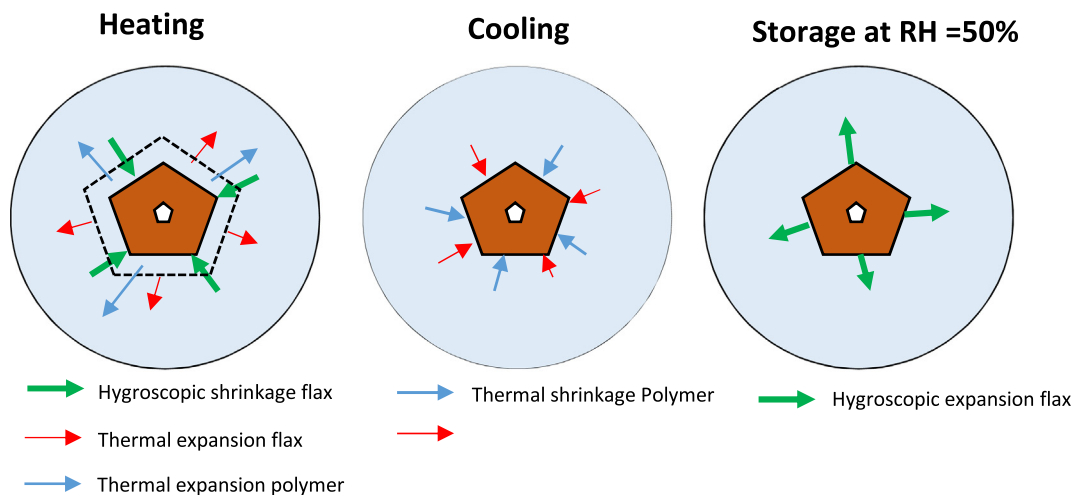


Fig. 5. Principle of residual stress generation at the natural fibre/polymer matrix interface. The thickness of arrows is proportional to the magnitude of stress. During heating, the hygroscopic shrinkage of the natural fibre occurs with higher magnitude than the thermal expansion of the fibre or polymer. The dotted line represents the initial position of the fibre prior to heating/drying. During cooling, the thermal shrinkage of the fibre and matrix occurs, and during storage, the hygroexpansion of the natural fibre induces large hygroscopic compression stresses at the fibre/matrix interface.

Adapted from [94] with permission from Elsevier.

Table 2

Coefficient of thermal and hygroscopic expansion of different fibres and polymers.

	Carbon fibre	Glass fibre	Flax fibre	Polypropylene
Radial thermal expansion coefficient $\alpha_{f,T}$ ($10^{-6}/^{\circ}\text{C}$)	18 [92]	5 [92]	78 [82]	120 [93]
Radial hygroscopic expansion coefficient $\beta_{f,R}$ ($\epsilon/\Delta m$)	–	–	1.14 [94]	–

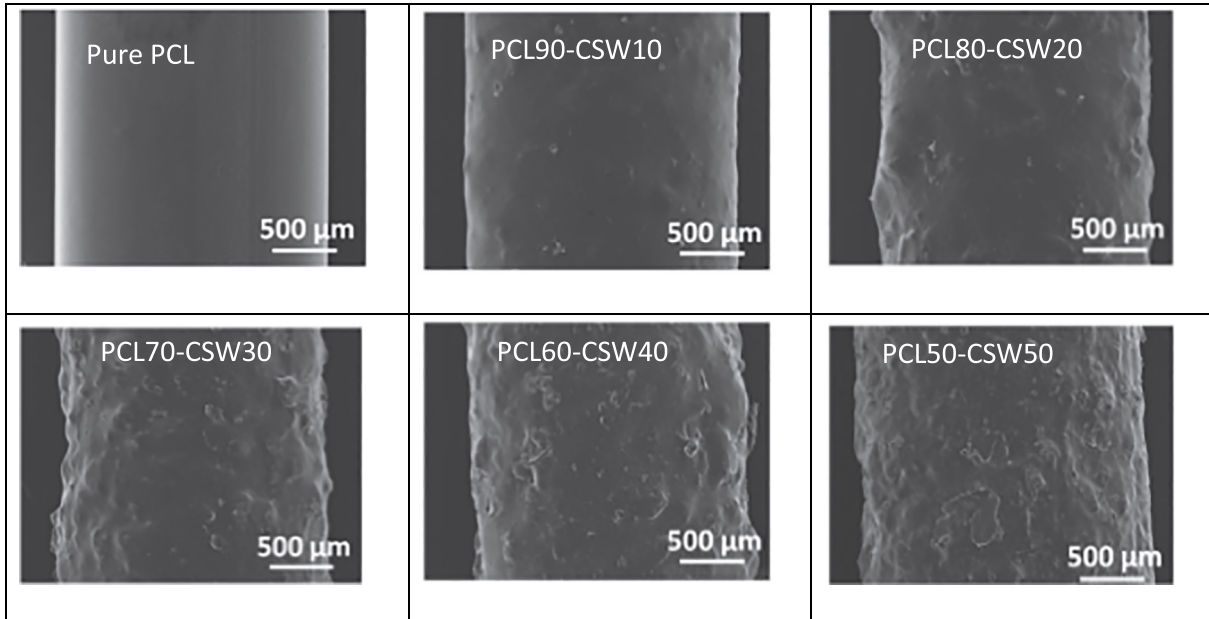


Fig. 6. Evolution of filament surface roughness with fibre content with PCL/Cocoa Shell Waste (CSW). Increasing fibre content induces filaments with a rough surface. Adapted from [80] with permission from Wiley.

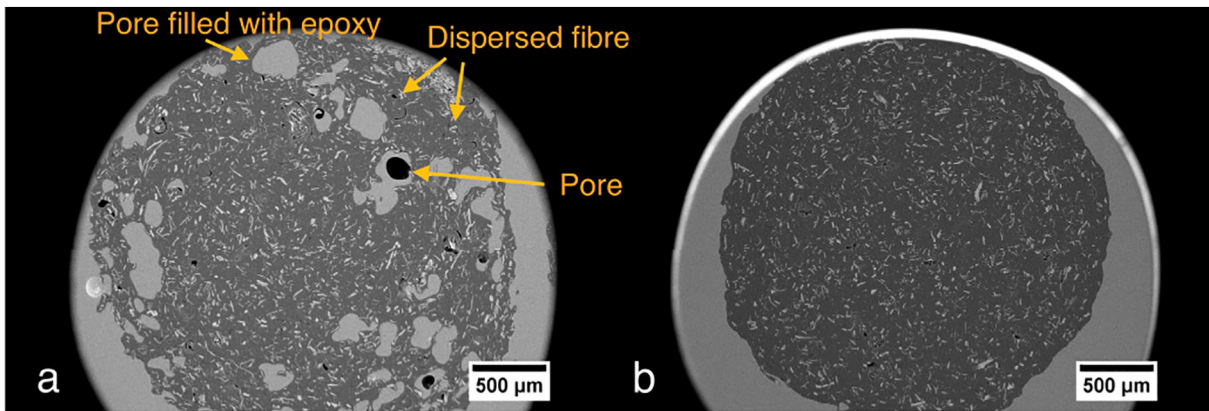


Fig. 7. Example of the microstructure of (a) extruded filaments with TMP fibre of 400 µm length and 38 µm width (b) and two subsequent extrusions of TMP/bioPE biocomposite. The subsequent extrusion leads to a shorter fibre, better homogenization, and lower porosity content. Adapted from [79].

(i.e. in powder form) to manage the viscosity of the biocomposite and reduce fibre agglomeration [80,114]. For example, Zhao et al. [114] have shown that the complex viscosity of Wood/PLA composites is reduced from 1.683 Pa·s to 1.549 Pa·s when the poplar fibre length decreases from 850 to 2360 µm to 180 µm and below. The authors state that the rheological behaviour plays a significant role in the 3D printing process as low viscosities at high shear rates are required for easy and low energy extrusion, but high zero-shear viscosities are also required so that the extrudate retains its shape once it is out of the nozzle and deposited. An optimum viscosity for an extrusion-based hydrogel 3D printing system is reported to be approximately

100–10,000 Pa·s [115]. The available literature has indicated that natural fibres have a low dimension with spheric cork particles between 272 and 733 µm [104], rice flour from 100 to 150 µm [116], hemp powder from 75 to 180 µm [96] and aspect ratio from 1 to 7 [90], bamboo fibres with a length from 627 µm to 827 µm, diameter from 134 to 189 µm and L/d between 4.12 and 4.72 [99], flax fibres with a length of 355 µm, diameter of 42 µm and L/d of 8.68 [99], TMP fibres with a 400 µm length and 38 µm diameter [108], Cocoa shell with a mean diameter of 50 µm [80], wood saw dust of 14 µm–237 µm [74,81,107], and flax shives with a median diameter of 162 µm and 20–650 µm for flax fibres [58].

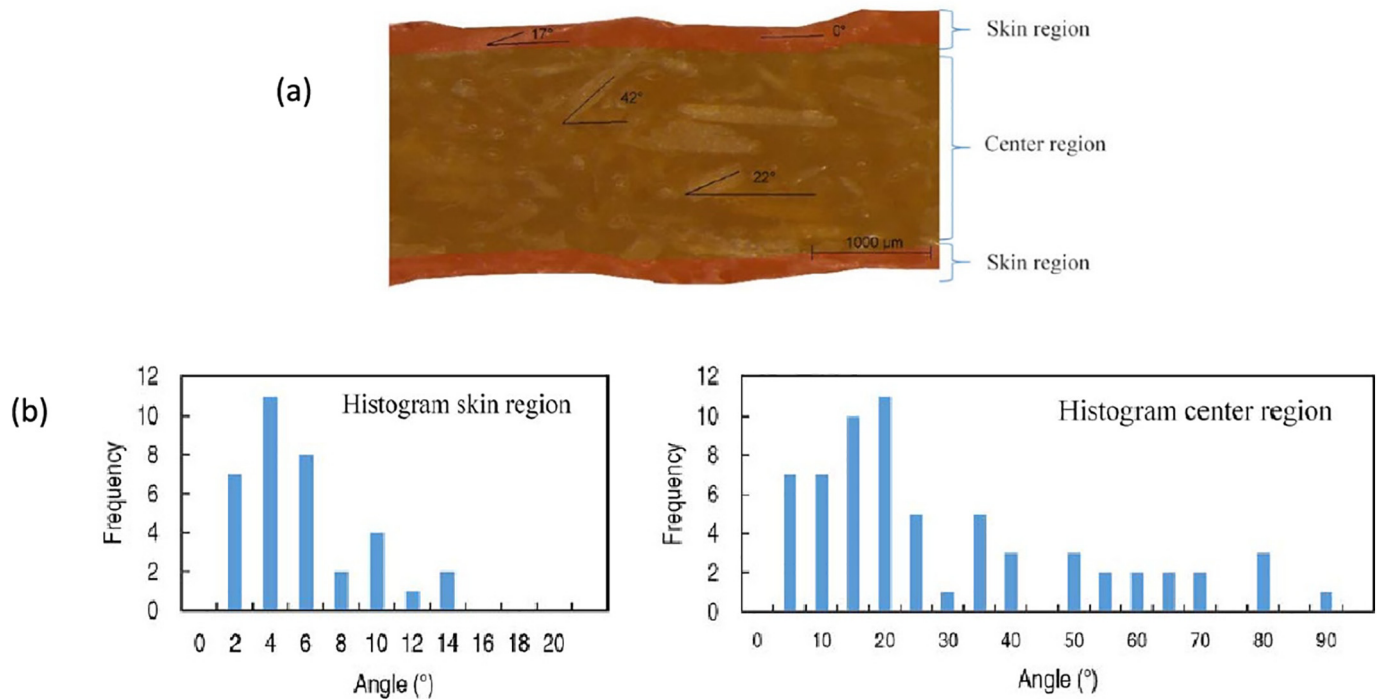


Fig. 8. (a) Microstructure of Bamboo/PLA filament showing skin and centre region due to a distribution of the orientation of the bamboo fibres. Bamboo fibres with $L = 713 \mu\text{m}$, $d = 153 \mu\text{m}$ and $L/d = 4.67$. (b) Distribution of the bamboo fibre angle showing the skin/core effect. Adapted from [99] with permission from Elsevier.

The effect of fibre size on 3D printed biocomposite porosity content is still rare. Powder-like bamboo fibres yield a porosity amount of 3.6% as against 0.3% for fibre-like geometry [99]. However, these results need to be confirmed as a change of PLA plasticizer can also affect the trend with no distinguishable effect of the fibre geometry on the porosity level.

In general, the tensile modulus of reinforced filaments is higher than that of pure polymer, while the rupture properties are lower due to insufficient fibre L/d and weak dispersion. For example, Depuydt et al. [99] have shown an increase in tensile modulus from 1.3 to 2.4 GPa by adding 15% flax or bamboo fibres at the same time as the strength is reduced from 31 MPa to 23–30 MPa. A L/d ratio lower than the critical L/d in the sense of Kelly-Tyson's equations [57] does not allow the stress to be transmitted efficiently to the fibre. For Bamboo fibre-reinforced PLA biocomposites, the authors found a critical L/d of 35.3 that was drastically above the real aspect ratio. From this perspective, fibres could be considered defects that introduce stress concentrations. The low interfacial shear strength between fibre and matrix and the high porosity of the filament significantly reduce the properties of the filament. Filgueira et al. [108] have shown that enzymatic modification of TMP fibres slightly increases the tensile strength of PLA composites filaments.

Filament production is a key step in the additive manufacturing cycle; any defects that occur at this stage (e.g. porosity) are transferred to the printed samples [117]. Coppola et al. [96] claim that the tensile properties of filaments and 3D-printed parts are similar, particularly in terms of stiffness. This is confirmed by the work of Le Duigou et al. [29] where the stiffness is similar between tests on filaments vs. tests on 3D-printed samples of wood/PLA/PHA biocomposites. In addition, when printed in the 0° direction (i.e. in the direction of the filament), the tensile strengths are similar. Printing at 90° to the longitudinal direction evidenced a 25% reduction in strength, which is indicative of the anisotropy of the filaments and the overall anisotropy of the sample. Thus, in wood fibre/PLA/PHA biocomposites, the fibre orientation follows the printing orientation of the filament.

Milosevic et al. [97], on Hemp and Harekeke recycled PP, showed a reduction in stiffness (–6 to –35%) and strength (around –60% for hemp and –30% for Harekeke) of 3D-printed tensile samples compared to filaments. This is due to the microstructure of the print showing poor bonding between the layers and the presence of stress concentration around the fibres.

3.2. Mechanical properties of natural fibre-based 3D printed biocomposites

The literature indicates that the mechanical characterization of 3D printed biocomposites has not been conducted in a systematic manner. Most articles have evaluated the capacity to manufacture bespoke filaments and have assessed printability by generating demonstrators [118]. The present article proposes an overview of the literature on the tensile properties of natural discontinuous and continuous fibre-reinforced biocomposites manufactured using FFF (Fig. 9a). Among the natural fibres examined are hemp fibres [78,96–98], hemp hurds [90], flax fibres [119] and shives [58], jute fibres [77,120], wood fibres [29,74,118,121], wood flour [81,102,110], waste macadamia nut shell [111], Harekeke fibres [96–98], rice straw [116], coconut fibres [105] and bamboo flour [101].

Fig. 9a, b, and c capture the data regarding tensile stiffness and strength provided by about 110 articles on printed natural discontinuous and continuous fibre composites, their synthetic counterparts, and natural discontinuous and continuous fibre composites manufactured by conventional processes (i.e. injection and compression moulding). The results of all the collected data, as presented in Fig. 9a and b, indicate a very scattered distribution profile. This is due to differences in the choice of materials and formulation (polymer, fibre type, fibre content - among others) but also to different processing parameters and printers.

In addition, it should be noted that there are currently no specific standards for the design of 3D printed mechanical samples. Even a

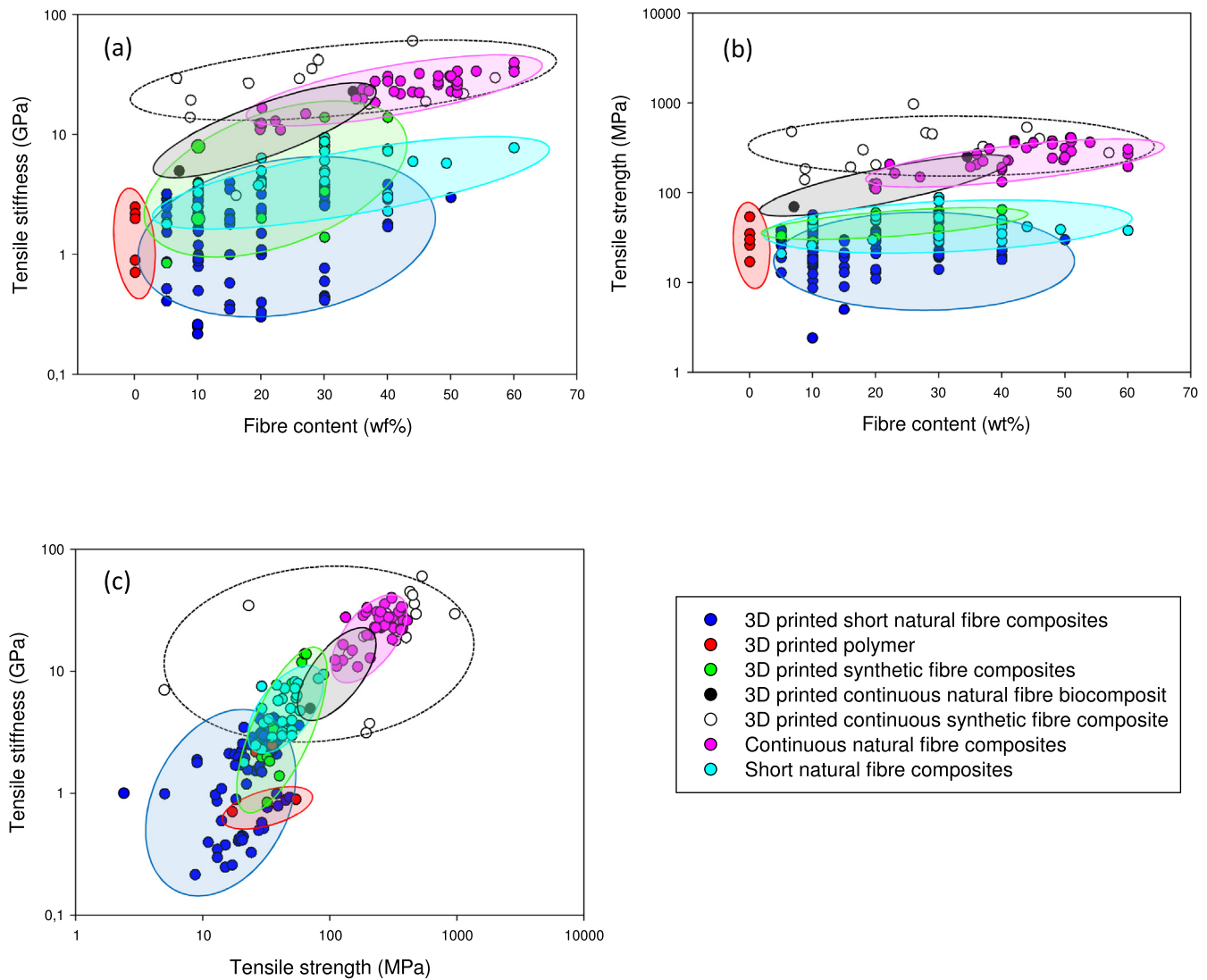


Fig. 9. Literature review on the tensile properties of natural fibre-based biocomposites manufactured by 3D printing. Stiffness (a) and strength (b) as a function of fibre content; (c) Stiffness as a function of strength of 3D printed pure polymer, short and continuous fibres natural fibre composites and conventionally manufactured short and continuous fibres natural fibre composites (injection, compression moulding) [29,56,58,68,74,75,77–81,90,96–99,101–105,110,111,116,118–150].

standardized sample geometry influences the performance measured on a pure polymer [151] or a continuous fibre composite [152].

Compared to pure polymers (Fig. 9a, b, and c), the printing of natural fibre-reinforced biocomposites results in a slight increase in the stiffness of the biocomposites combined with a general decrease in their strength [77,80,90,96,97,104,105,116,121].

Safka et al. [105] have shown that ABS/Coconut biocomposites exhibit a slight increase in tensile modulus (+6%) and a drastic reduction in strength (−50%) and strain (−15%) compared to a neat matrix. Dong et al. [121] have found a reduction of about 60% in tensile strength, about 55% in Charpy impact strength, and about 60% in flexural strength. The addition of cork powder to PLA also reduces the tensile modulus, strength, and impact strength of printed PLA biocomposites [104]. Zander et al. [110] have found an increase in tensile modulus of 60% for PP/10% wood flour and 20% for PP/cardboard compared to pure PP, respectively. They also observed a decrease in tensile strength of 7 to 20% for PP/paper waste fibres and on PP/cardboard fibres. Xiao et al. [90] observed a reduction in tensile strength of about 20% while mixing hemp hurds in a PLA matrix. Guessasma et al. [122,124] have reported a reduction in stiffness (7–10%) and strength (10–20%) for PLA/hemp and PLA/wood compared to pure PLA. They also point out that the

wide dispersion of results, within a range of 18%, could be attributed to the natural variability of hemp or it could also be due to an inhomogeneous distribution of fibres within the filament.

In conclusion, the available data indicate that there are only rare cases where the addition of natural fibres shows an improvement in all mechanical properties of the biocomposites. One such exception can be found in the work of Tarrès et al. [123], on a compatibilized bioPE reinforced with thermomechanical pulp (TMP) fibres, which showed an increase in stiffness and strength with the addition of 10 to 20% of fibres. It is assumed that this exception is due to the combination of a better bond strength of the fibre/matrix interface and a relatively high interfacial surface area (the initial length of the fibres is 1.5 mm, and their diameter is 33 μm).

The role of natural fibres as a potential reinforcement should therefore be examined. For instance, natural fibres could be better positioned as “fillers” used to valorise biobased feedstock and biological waste by reducing the content of polymer and potentially reducing cost [116]. Natural fibres can also increase the biobased content in targeted applications, while their aesthetic properties can be applied to bring original qualities to the printed design (colour, roughness). The porous characteristics can be similarly used to reduce the density of the composite

[104]. However, what is increasingly evident is that due to their mechanical properties, it is difficult to apply natural fibres to a semi-structural application.

Printing and slicing parameters have been demonstrated to play an important role in the mechanical performance of 3D printed parts using FFF [153] and consequently, they have a great impact in the production of biocomposites. These parameters include infill percentage, printing pattern, raster angle, printing height, printing orientation, printing/bed temperature, and printing speed.

In terms of temperature, Guessasma et al. [122], have shown that wood-based biocomposites exhibit stable tensile properties over a range of 210 to 250 °C, while Hemp/PLA biocomposites have shown an increase in performance over the same temperature range (210 to 250 °C) [124]. Yang et al. [84] have shown a slight decrease in tensile and flexural properties when the extrusion temperature is between 200 and 230 °C, but an increase in compressive strength (+15.1%) and internal bond strength (+24.3%). The higher extrusion temperature has shown better compatibility at the fibre/PLA interfaces and good adhesion between the extruded filament segments, while at the low printing temperatures, the loss of tensile performance (approx. 20%) is similarly explained by a lack of cohesion between the filaments.

To our knowledge, no studies have been performed on the effect of printing speed on the performance of biocomposites based on natural fibre. Based on their review work, Mazzanti et al. [117] have argued that the reduction in high-temperature residence time implied by faster printing speed may prevent the degradation of natural fibres.

In regard to printing pattern and infill, research by Vigneshwaran et al. [125] shows that changing the filling percentage from 30 to 90% multiplies the tensile strength and stiffness by a factor of 2 and 1.5 respectively for wood/PLA biocomposites. The printing pattern, whether rectangular, triangular, or hexagonal, does not seem to influence the final properties of biocomposites [125].

Independent of the printing pattern, reducing the layer height generally results in better cohesion and tensile properties of the printed biocomposite. For instance, by decreasing the layer height from 0.3 to 0.05 mm, Ayrlimis et al. [126] have shown an improvement in tensile strength from 20.5 to 35.5 MPa and stiffness from 2567 to 3542 MPa. This finding confirms similar work by Le Duigou et al. [29] and Dong et al. [121] on comparable wood/PLA/PHA biocomposites. The latter have also tested the role of shell number and found that 2, 4, and 6 shells slightly increased the tensile strength of Wood/PLA/PHA biocomposites because the filaments printed on the inside of the shell are oriented along the perimeter of the specimen and therefore in the direction of the tensile load.

Liu et al. [103] have examined the effect of printing orientation (0, 90, ±45 and 0/90°) on the tensile strength of sugarcane bagasse fibre/PLA biocomposites. Longitudinal printing at 0° was the best solution, with a 7% improvement compared to the cross solution (±45 and 0/90°) and 20% improvement compared to transverse printing at 90°. This trend continued to be observed when the fibre content was increased. Le Duigou et al. [29] have observed more drastic changes between 0 and 90°, which also depend on the distance between the printed filament. Thus, printing at 0° could exhibit two (2×) or three times (3×) higher strength than printing at 90°.

Interestingly, Torrado-Perez et al. [77] have shown that depending on the test direction (XYZ or ZXY plane), the effect of the natural fibre is different with a greater decrease in the out-of-plane direction compared to the in-plane direction. Due to the high porosity of the Jute/ABS filament, a rupture of the trans-filament is observed (Fig. 10).

Compared to conventional manufacturing (injection or compression moulding), 3D printed short natural fibre biocomposites have generally lower tensile properties (Fig. 9 a, b, and c) [108]. Le Duigou et al. [29] experienced a 44% reduction in stiffness and a 30% reduction in strength compared to compression moulding for wood/PLA/PHA. Safka et al. [105] have found a 50% reduction in stiffness and strength of ABS/cocunut fibres compared to injection moulded counterparts. Tarrès et al.

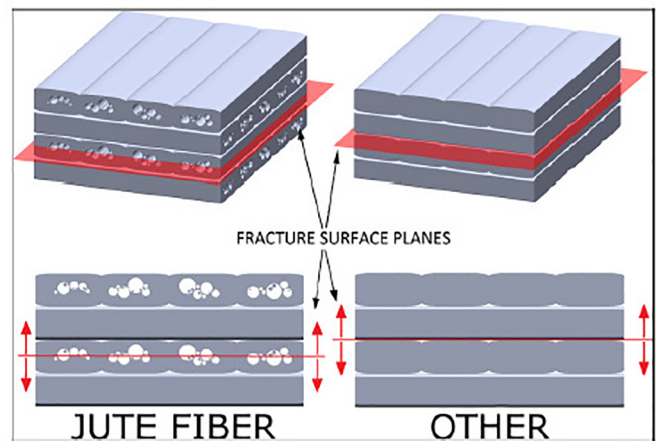


Fig. 10. Schematic view of the fracture plane for jute fibre-reinforced ABS compared to neat ABS [77]. A cohesive fracture within one layer and more specifically within jute fibre bundle is observed for jute/ABS. The fracture occurs in the interlaminar area for neat ABS.

[123] demonstrated that Thermomechanical Pulp (TMP)/BioPE biocomposites have lower properties than their injection-moulded counterparts with similar fibre content (10–20%). This is indicated by a reduction of about 40% in modulus (even for neat polymer) and about 45% in strength with a fibre content of 10% and, interestingly, about 10% with a fibre content of 20%. This significant difference is attributed to the microstructure of the 3D printed parts with poor adhesion between the printed layers resulting in a significant increase in the porosity content [123].

Comparison of 3D printing of flax fibres or shives/PLA, PLA/PBS or PBS with injection-moulded samples shows a reduction in the stiffness of the composite between 5 and 25% depending on the matrix and a reduction of between 10 and 55% for the strength [58]. However, the work of Daver et al. [104] shows that PLA/cork with 3D printing is only slightly lower than the compression-moulded counterparts. Unfortunately, no clear explanation for these results was presented in the article although it is speculated that the low cork content could be the culprit.

The comparison with short synthetic fibre composites shown in Fig. 9 a, b, and c demonstrates that there is a global trend towards lower stiffness and tensile strength for natural fibre composites compared to synthetic fibres, especially when carbon fibres are used [128,131]. This is logical and can be explained by the intrinsic difference in properties between types of reinforcement. Based on the current state of the art, short glass fibre-reinforced composites, which are often cited as the target for the mechanical properties of biocomposites [56,139], have similar stiffness but slightly higher strength (compared to a similar fibre content) [78,98,130]. However, from a mechanical point of view, the comparisons made in the literature are questionable because the weight fraction of the fibres is mainly considered due to technical issues (e.g. viscosity) whereas reinforcement is a volume effect.

When analysing the current literature, the moderate tensile properties of 3D printed natural fibre composites can be explained by several parameters:

- Low fibre content to maintain the viscosity of the composite at a relatively low level (generally less than 30 wt%). Filaments with a higher natural fibre content do not flow uniformly through the nozzle and generate poorly printed parts that are not evenly filled with material [74]. In addition, an increase in melt viscosity would require higher power for extrusion through the nozzle [117]. Most of the published work deals with a fibre content between 5 and 20%. Printing of the composites through a 1-mm die showed that from a fibre content of 20 wt%, sporadic semi-blockages of the die occur, leading

to slip-stick extrusion [75]. Semi blockage could be reduced by using a larger extrusion die, but it also reduces the definition of the part [127]. The design of an appropriate die is therefore of great importance. Since the 3D printing process cannot provide a high shear rate, the selection of a suitable polymer matrix with adequate viscosity is essential to control the printability of the material. Hence, biocomposite filaments made from the bioPE polymer were not suitable for 3D printing [123]. Conversely, a low viscosity promotes warping and shrinkage problems during the 3D printing [79].

- A low aspect ratio ($L/d < 10$) results in a low interfacial surface area. Initially assembled in bundles in the plant (Fig. 1), the natural fibres exhibit an aspect ratio that evolves during the process with a high shear rate like extrusion [140], but the change in L/d has not yet been demonstrated for 3D printing. A low aspect ratio (L/d) of the reinforcement, lower than the critical aspect ratio as evoked by Kelly-Tyson's equations [57], implies that the load transfer at the fibre/matrix interface is not efficient. This leads to debonding rather than fibre breakage. For example, Depuydt et al. [99] have calculated the average stress in the flax fibre of 75 MPa assuming interfacial shear strength of 9 MPa, with an L/d ratio of 8. This stress is theoretically only 0.14% of the maximum stress applicable to the fibres in a continuous fibre composite and therefore confirms interface debonding rather than effective stress transfer. Milosevic et al. [97] have shown that Harekeke fibres with a higher L/d ratio than hemp fibres have a better reinforcement efficiency. The low aspect ratio is often chosen in accordance with the diameter of the nozzle, which limits the size of the reinforcement. If larger particles were used, there would be more clogging [74]. Again, further developments of the printing device are needed to meet the requirements of high-performance composites. An integrated extruder, bringing similar advantages of high strain rates, should be preferred in the near future.
- The moderate mechanical properties of the selected natural fibres generate a low reinforcing effect. As shown in Table 1, natural fibres have different mechanical properties depending on their microstructure and biochemical composition. Bast fibres such as hemp or flax are the result of a dedicated harvesting and yield a higher potential for composite reinforcement. In the current literature, wastes from industry or agriculture, such as wood sawdust, rice or coconut husks, are mainly used. Although they offer a cost-effective solution, their mechanical performance is inferior (Table 1), while their environmental benefit should be confirmed by a standardized life-cycle analysis.
- The high porosity content of the printed samples is attributed to the combined effect of the low pressure exerted between the layers during the printing process and the heterogeneous temperature in the different regions of a printed part. First, the porosity of printed biocomposites is higher than that of pure filaments and increases with fibre content, which indicates the need for further work on natural fibre/polymer rheology, fibre/matrix compatibility, and process-induced compression [79,90,123,127]. Porosity could be reduced by vacuum drying the natural fibre before printing [99] or by controlling the temperature and humidity during printing [97].

On printed samples, Guessasma et al. [122] showed on Hemp/PLA biocomposites that during printing, the temperature difference between the peak and the ground can reach 95 °C at a printing temperature of 250 °C due to convective and conductive heat dissipation. This temperature difference gives porosity located between the filaments (size ≈ 1 mm), inside the filaments (size ≈ 100 μ m), and in the zone of abrupt change of trajectory (size ≈ 1 mm) [122]. Porosities are generally organized in a network that represents the majority of voids within the biocomposite (Fig. 11a). It could be suggested that printing chambers heated by active convection might be able to maintain more consistent temperatures throughout the part. In another study, the authors

also stated that an increase in porosity from 3.15% to 8.7% was observed in the temperature range of 210 to 240 °C due to the change in the filament cross section that is not compensated for the print height and filament build-up at the nozzle [124] (Fig. 11b).

Layer height also influences the microstructure and porosity level of biocomposites. Le Duigou et al. [29] and Ayrilmis et al. [126], have demonstrated the effect of layer height on the porosity content of the wood/PLA composite. An increase in layer height from 0.05 to 3 mm induces a greater amount of porosity (Fig. 12), an increase in water absorption, and a reduction in tensile properties (30% modulus and 40% strength) [126].

Generally, the natural short fibre-reinforced biocomposites currently used in FFF yield to moderate mechanical properties that prevent them from being applied in semi-structural applications. Therefore, further research is needed to overcome the weaknesses identified in both processing methods and material formulation.

3.3. Future trends in 3D printing of natural fibre biocomposites

A promising recent strategy is to print continuous natural fibre composites by in-nozzle impregnation [120] or using pre-impregnated filaments [119] using modified printers. Fig. 13a and b show a photograph of a broken area of a unidirectional printed sample of continuous jute fibre yarns with in-nozzle impregnation of PLA and a unidirectional printed sample of continuous flax fibre yarns/PLA with pre-impregnated filaments. The rupture modes were different with a multi-scale debonding for the Jute/PLA, thus testifying to poor load transfer and incomplete wetting. Unidirectional Flax/PLA evidenced a typical rupture mode compared to unidirectional composite materials [146] with transverse cracks followed by propagation along the tensile axis. Fibre breakages are also observed, although numerous pull-outs of flax fibres inside the yarn could also be observed.

The mechanical properties of biocomposites including continuous jute or flax yarns have far exceeded the mechanical properties of natural discontinuous fibre composites (Fig. 9a, b, and c). The pre-impregnation of the natural fibres has made it possible to reach significantly better performance. The overall performance of PLA/Jute (6% by volume) composite reached a stiffness of 5.11 ± 0.41 GPa and a strength of (57.1 ± 5.33) MPa while PLA/Flax (30% by volume) had a stiffness (E_L) of 23.3 ± 1.8 GPa and a strength of 253.7 ± 15 MPa.

The difference between these results relied on i) the lower linear density of flax with 68 tex compared to 500 tex for jute yarn favouring a homogeneous distribution of the reinforcement within the composite, impregnation during the filament manufacturing and printing processes, reducing printing defects (Fig. 13c); ii) Flax fibres have much better mechanical performance than jute fibres (see Table 1); and iii) a higher fibre content can be achieved with pre-impregnated flax yarns compared to in-nozzle impregnation (30% vs. 6%). In addition, 3D printed continuous flax/PLA biocomposites present competitive tensile stiffness and strength as biocomposites of similar fibre content manufactured by thermocompression (Fig. 9a, b, and c).

Compared to composites reinforced with continuous synthetic fibres (Fig. 9a, b, and c) with similar printing technology (i.e. pre-impregnated filaments), two cases have to be analyzed. First, compared to continuous carbon fibre composites, the performance of continuous flax fibres is radically inferior in terms of stiffness and strength [132,134,154]. However, the comparison of mechanical performance with continuous glass/PA composites [134,135] is encouraging because a similar range of stiffness can be achieved if continuous flax biocomposites are printed. Therefore, semi-structural or structural applications where a glass/composite is used, especially for stiffness-based design, should be open to continuous natural fibre biocomposites.

Future strategies to achieve higher performance for biocomposites printed with a continuous natural fibre may include the following avenues. At the material scale, optimized filament production using a low twisted yarn combined with low linear weight is of great promise.

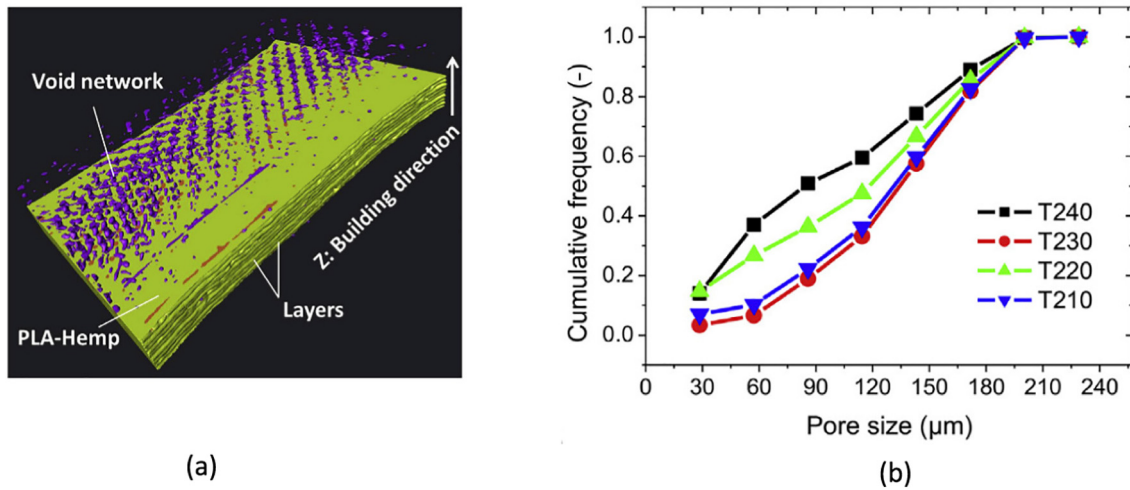


Fig. 11. (a) Perspective view obtained by microtomography showing the formation of void in a form of network in the printed structure and (b) the pore size distribution in Hemp/PLA biocomposites for different printing temperature. Increasing the temperature from 210 to 240 °C induces a higher frequency of low size pores within Hemp/PLA biocomposites. Adapted from [122] with permission from Elsevier.

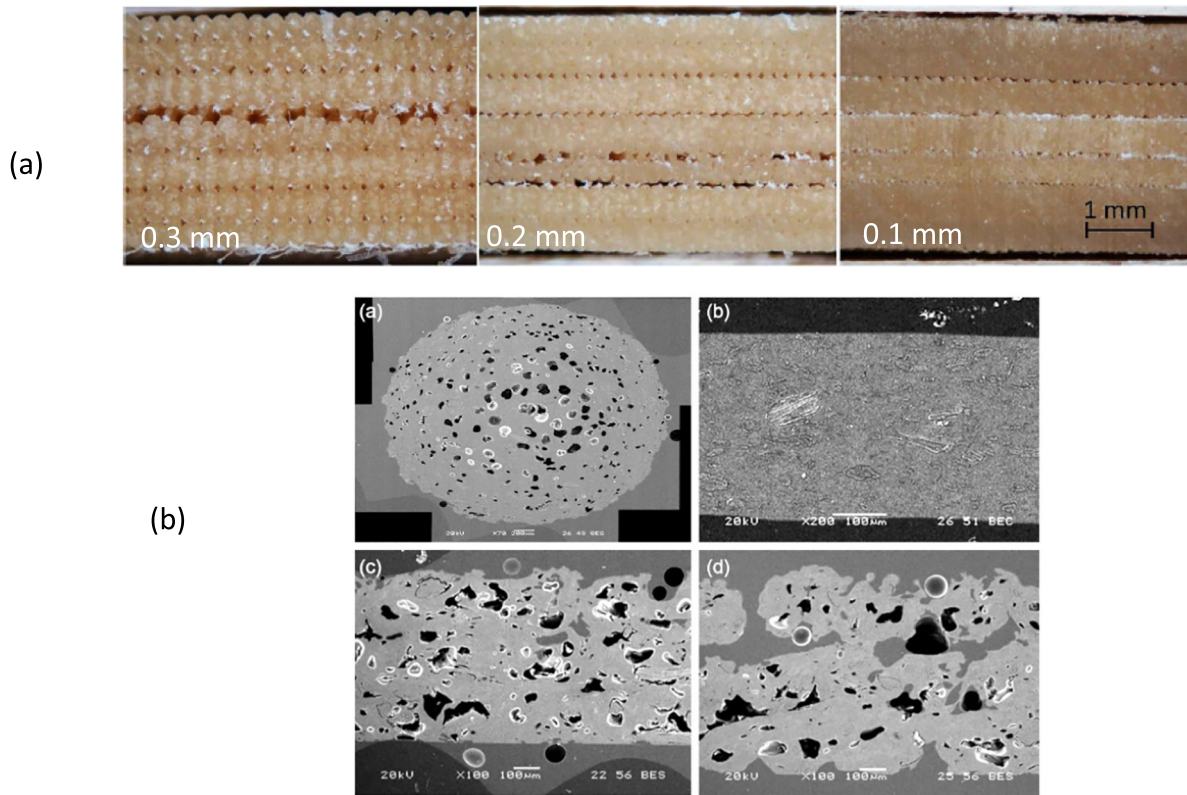


Fig. 12. a) Effect of layer height on wood, 0.3, 0.2 and 0.1 mm [126]. Higher layer height set by the slicer generates a microstructure with higher porosity content. b) SEM micrography of printed wood/PLA biocomposites with raw filament cross-section, compressed printed samples and various filament thickness. Adapted from [29,126] with permission of Elsevier.

Baets et al. [155] have shown that the overall performance of composites decreases when the yarn undergoes strong twisting due to load mis-orientation and lack of impregnation. In addition, commingled natural fibre/polymer yarns should also be proposed in order to improve their impregnation during the production of filaments and their printability. Finally, the selection of the reinforcing quality is of great importance to produce high quality printed biocomposites that should target structural or semi-structural applications. This may also include hybrid

fibre formulations (natural and synthetic) and adapting fibre selection to the intended application.

A potential improvement in the performance of 3D-printed natural fibre composites could occur through the development of customized and cost-effective processing devices. This includes, for example, a modified nozzle with an integrated extrusion system with pelletized biocomposites that increases fibre content, printing speed, and may also reduce processing costs [114]. Large-scale additive manufacturing

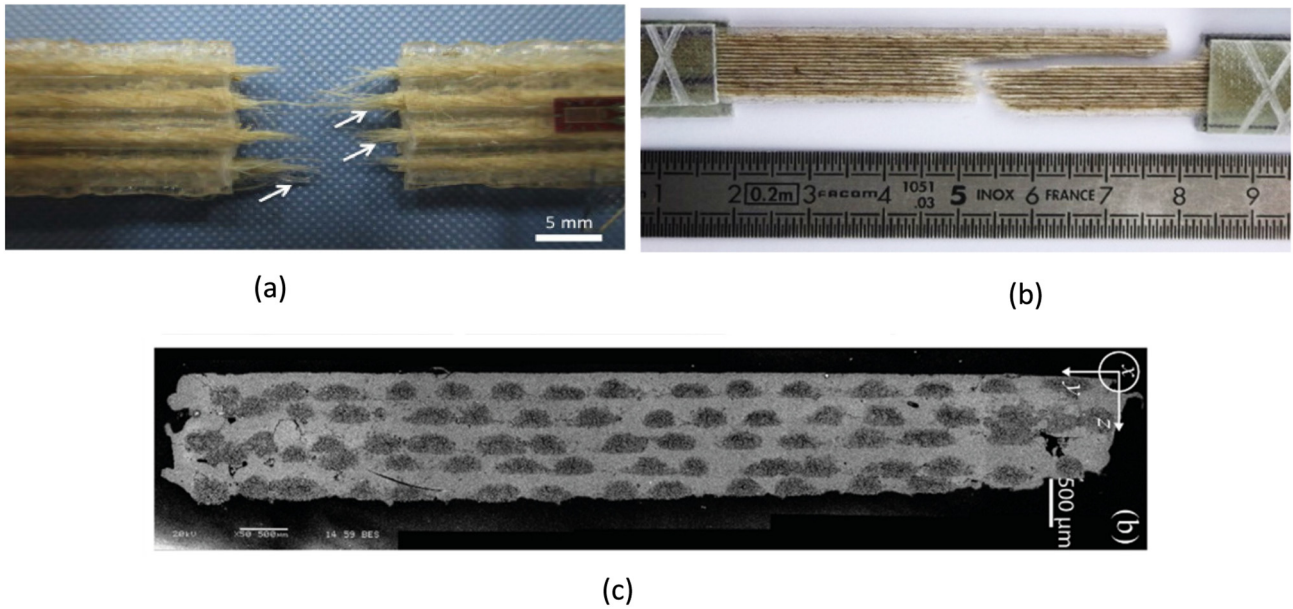


Fig. 13. (a) Fractured continuous unidirectional jute fibres/PLA sample printed with in-nozzle impregnation. Lack of jute yarn impregnation is observed with numerous fibre debonding. (b) Fractured continuous unidirectional flax fibre/PLA sample printed with pre-impregnated filaments. Typical rupture mode is observed with transverse crack followed by propagation along the tensile axis. (c) SEM micrograph cross section of Flax/PLA composite microstructure. Adapted from [119,120].

for wood/PLA biocomposites (Fig. 14) has recently been developed by Zhao et al. [114]. The main advantages of this approach are a high deposition rate up to 50 kg/h and a high building volume ($\sim 27 \text{ m}^3$), which reduces treatment time and cost. In addition, instead of 3-axis printing (Cartesian printing), they have implemented a 6-axis printing (polar printing method), which makes it possible to print even more complex shapes. Beyond the additional degrees of freedom of movement of the 6-axis printing configuration, automated fibre placement (AFP) with a 6-axis industrial manipulator (robot arm) could also be achieved [145], but the additional cost would have to be questioned. Currently, this complex implementation requires significant costs related to the integration of a tailor-made system; it may even require additional technical steps compared to a gantry style 3-axis printer (e.g. additional compression).

However, the ability to use the 6 degrees of freedom in combination with specialized end-effectors capable of providing additional placement and processing capabilities, such as a cutting device, opens the possibilities of increased control over filament placement and more precise manipulation of the microstructure of the material. These additional capabilities should open new opportunities for the manufacture of high-performance biocomposites. For example, the 37%vol. PP/Flax biocomposite made with AFP followed by thermal compression has a tensile modulus (E_1) of $28.9 \pm 1.9 \text{ MPa}$ and a tensile strength of $183 \pm 8 \text{ MPa}$. These values are similar to those of thermocompressed biocomposites, but this new process provides the ability to accurately control fibre orientation (and fraction), the lay-up thickness, and the overall architecture.

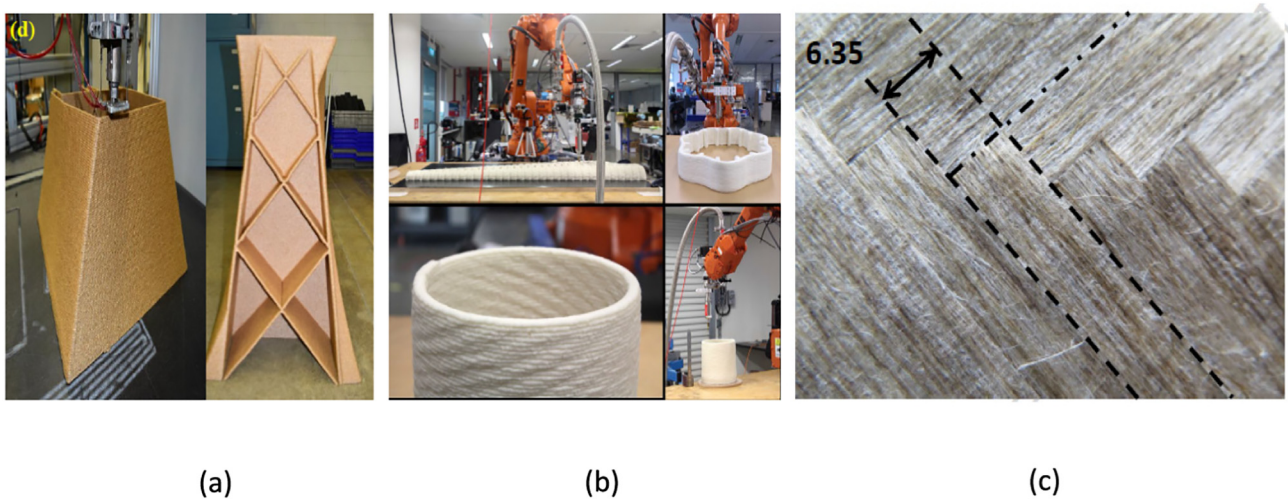


Fig. 14. (a) Large scale printing process with poplar/PLA composites. Adapted from Zhao X, Tekinalp H, Meng X, Ker D, Benson B, Pu Y, et al. Poplar as biofibre reinforcement in composites for large-scale 3D printing. ACS Appl Bio Mater 2019. doi: <https://doi.org/10.1021/acsabm.9b00675>. Copyright (2019) American Chemical Society. (b) Chitosan/wood flour/cellulose composites. Adapted from [156]. (c) Picture of $\pm 45^\circ$ PP/Flax laminate composite manufactured with Automated Fibre Placement (AFP). Each tape width is 6.35 mm. Adapted from [145] with permission of Elsevier.

4. Natural fibre biocomposites for 4D printing

4.1. Principle

4D printing is defined as the ability of 3D printed materials to actuate when an external stimulus (e.g. temperature, moisture, pressure, electricity, pH, light) is applied [21]. For shape-transformation materials, two subclasses are discussed in the literature: shape-changing materials and shape-memory materials [32,157]. Shape memory refers to the ability of materials to “remember” and recover their original shape. This implies that the original shape can be deformed and fixed into a secondary form by an external physical force. This new shape is retained until a specific stimulus is applied that triggers the transformation of matter and its return to its original shape [3,32]. Shape Memory Polymers (SMP) achieve this via a dual segment system (elastic segment and transition segment [158], which allows them to be physically deformed but to return to their original shape under the effect of an appropriate thermal stimulus [159]. Shape-changing materials operate differently because it is the external stimulus that triggers the transformation from their original shape; then, the transformation is reversed when the stimulus is removed. Therefore, one can consider that the material oscillates between two states of equilibrium without the need for an external force, allowing multiple transformation cycles. However, the direction and amplitude of the movement are pre-programmed into the material structure [157]. The effect of humidity as a stimulus for shape-changing materials is a growing area of research for 4D printing systems [25,160,161]. Currently, hydrogels are the main active polymers used in 4D printing using moisture-triggered actuation. Hydrogels and SMP are often integrated with a non-swelling polymer or filament to produce moisture and/or temperature-sensitive materials. However, the stiffness of both hydrogels and SMPs is relatively low [12], which reduces their actuation authority.

This limitation can be overcome by a composite strategy, in which the soft gel or polymer is combined with a reinforcement. This includes composites using localized regions of two different polymers (one SMP and one non-reactive) [162–164], the use of shear-oriented cellulose fibres [25] or magnetically oriented stiff particles [165] to manipulate anisotropic swelling in hydrogels [25], or the creation of thermally activated shape-change bilayers using continuous carbon fibre and PLA or PEEK polymers [166].

Natural fibres are anisotropic and sensitive to moisture, and this is one of their main drawbacks when used for structural applications [16]. However, actuation in response to a stimulus by pre-programmed hierarchical structures, such as nastic fibrous motors [167], can provide a bio-inspired model useful for the functional gradation of natural fibres to develop hygroscopically induced morphing, namely hygromorphing. The hygroscopic actuation of pine cones [26,168] (Fig. 15), wheat awns [169], and other seed dispersal mechanisms [170] can provide valuable insights for biomimicry and developing novel material functionalities.

Their principle is based on a hierarchical bilayer microstructure composed of sclerenchyma and sclereids. Each of these tissues is organized as a bundle of single fibres where each fibre is architected as a concentric composite cylinder of different cell walls (similar to Fig. 1). The secondary cell wall, which is mainly responsible for the hygromechanical properties of the single fibre, is composed of oriented stiff cellulose microfibrils embedded in the hygroscopic hemicellulose/pectin matrix. Thus, the response (bending) of the pine cone is provided at the cell wall that gives way to tissue swelling. The bilayer assembly leads to a differential swelling between two layers connected to each other by a gradual interphase (Fig. 15 and [171]).

Currently, work has been conducted on wood [172–176], spores [177,178], and natural fibre-reinforced (flax, jute, coir, kenaf) polymer biocomposites called hygromorph biocomposites [8,15,26,168] (Fig. 15). These novel materials therefore belong to a category of smart materials that are frequently cited in recent reviews on 4D

printing [3,32,179–181]. Their design is currently based on adapted Bi-metallic theory for bilayers, derived from the hygro-elastic properties of each layer [182]. In this case, the variation of curvature between the initial and the final state of actuation (also named responsiveness) is

$$\Delta\kappa = \frac{\Delta\beta \cdot \Delta C \cdot f(m, n)}{t} \quad (1)$$

$$f(m, n) = \frac{6(1+m)^2}{3(1+m)^2 + (1+mn)(m^2 + \frac{1}{mn})} \quad (2)$$

With $f(m, n)$ a function depending on several variables such as $m = \frac{t_p}{t_a}$ with t_p and t_a are the passive layers and the active layer thicknesses, respectively. The active layer is considered as the swelling phase, while the passive layer is the non-swelling phase that is used to bring stiffness to the assembly. Then $n = \frac{E_p}{E_a}$ where E_p and E_a are the longitudinal tensile moduli of the wet passive and active layers, respectively. $\Delta\beta$ is the differential hygroscopic expansion coefficient between the active and passive layers. ΔC is the moisture content difference within the material between the testing environment and the storage state. Finally, t is the total thickness of the sample (active and passive layers).

4.2. Actuation properties of natural fibre-based 4D printed biocomposites

4D printing of hygromorph biocomposites is generally limited to off-the-shelf materials with principally wood floor/biopolymer filaments [28,29,183] provided by Laywoo® or Colorfabb®. Wood-derived cellulose fibres are also used in combination with a polyacrilamide matrix [25], although they cannot be considered as true natural fibres due to their extraction process.

Like biological structures, anisotropic hygro-expansion is targeted in hygromorph biocomposites. At the microscopic level, fibre orientation dictates the direction of expansion, and within the polymer composite, the fibres are oriented primarily during filament production rather than printing [29]. However, printing trajectories and the orientation of the raster pattern create oriented mesostructures in the printed structure that are of great importance in promoting complex actuation. Generating actuation with 4D printed hygromorph biocomposites is currently carried out with two design strategies: monomaterial printing and multi-material printing deposition (Fig. 16a, b, c, d, e, and f).

The monomaterial approach is based on the anisotropy of the material induced by the orientation of the fibres within the filament and the printing process itself. It presumes that the same printed material possesses different mechanical properties and different coefficients of expansion in different directions. In general, the stacking sequence follows an asymmetric lay-up, i.e. a bilayer microstructure. Differential swelling between layers, which leads to out-of-plane displacement, is the target of this approach. Among monomaterials, two sub-categories can be found: i) full material filling (Fig. 16a) [29], and ii) partial filling on both layers with variable distance between the printed filaments (Fig. 16b, c, and d) [183].

i) For full material filling, actuation is influenced by the differentiated orientation between the printed layers (Fig. 17a), the overlap of the filaments that controls the porosity content, the layer height, the order in which the active and the passive layers are printed in the bilayer, the total number of printed layers and the length to width ratio [29,184], and the orientation of the raster pattern printed.

Printing a raster pattern in the hygroscopic layer of 0 or 45° in relation to the main longitudinal direction in a bilayer strip generates either curvature or twisting response of the hygromorph. Thus, the hygromorph biocomposite actuates in the orthogonal direction according to the printing angle of the active layer [183].

Changing from positive to negative overlap during printing modifies the porosity content of a wood/PLA/PHA biocomposite from 8.4 ± 1.7 to

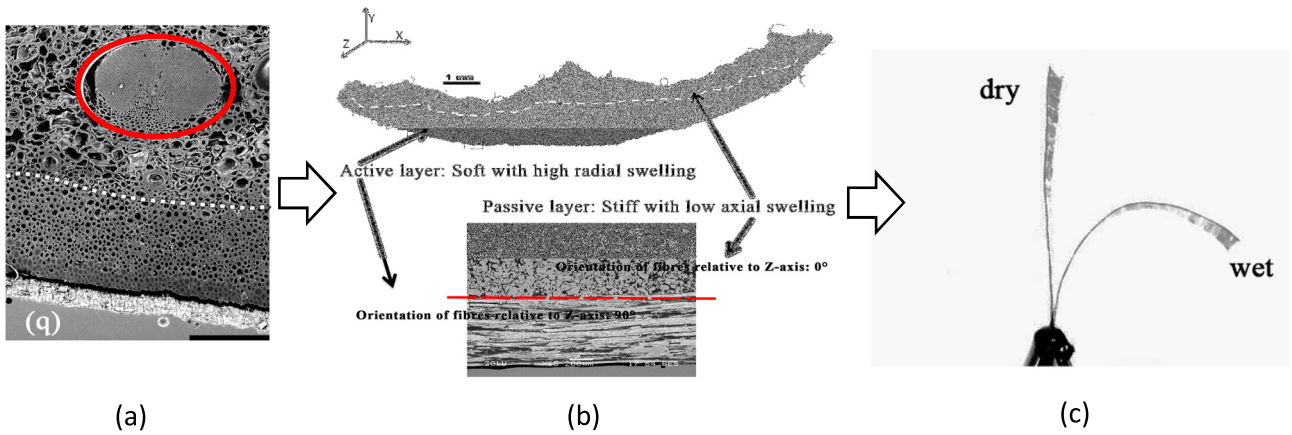


Fig. 15. Synoptic of biomimicry approach applied to develop novel features for natural fibres based on their moisture sensitivity and microstructure: hygromorphing. The source of inspiration is the microstructure of a pine cone scale from the gradual transition zone between two types of tissues (red circle and dash point line) (a) to the asymmetric or bilayer lay-up (b) where each layer possess different elastic and hygro-expansion properties. (c) The bio-inspired solution i.e. hygromorph biocomposites are based on the anisotropic hygroexpansion of natural fibre and the asymmetric lay-up similarly to pine cone. Adapted from [26,168] with permission of Elsevier.

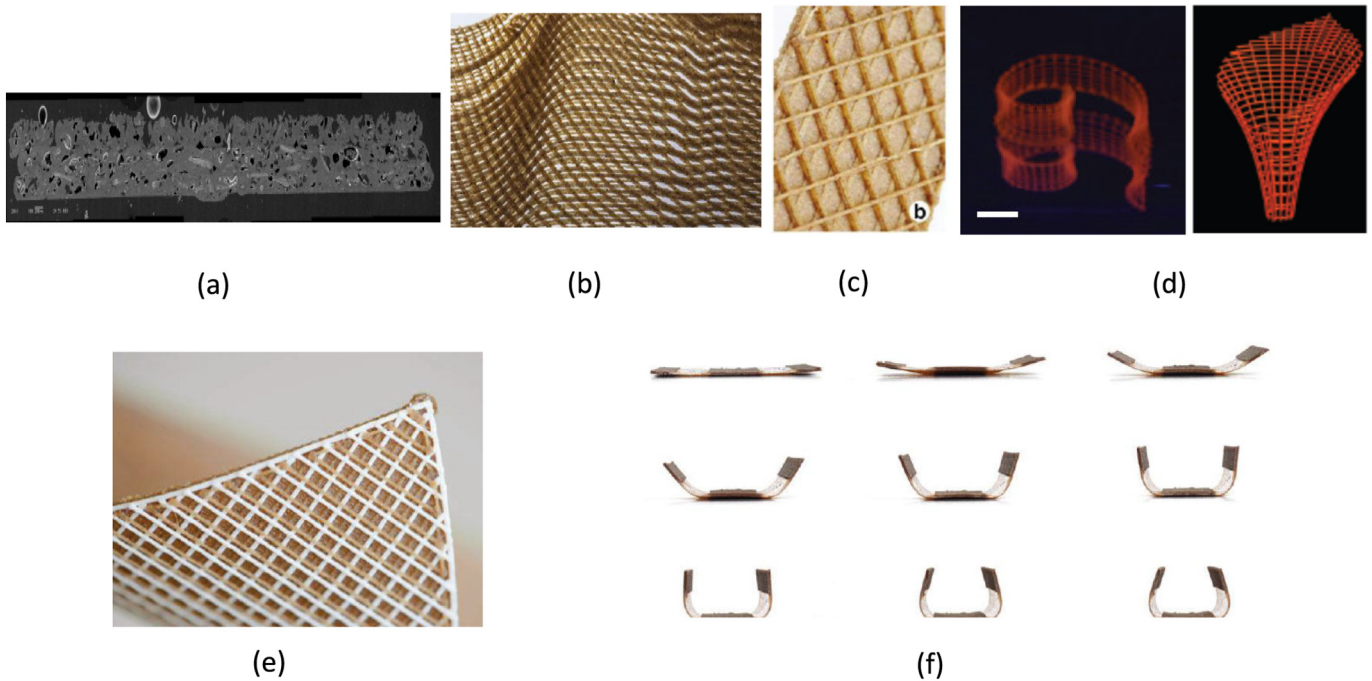


Fig. 16. Printing methodologies for hygromorph biocomposites. (a–d) Monomaterial option with wood/biopolymer and nanocellulose/hydrogel biocomposites. Adapted from [29] with permission of Elsevier, from [30] and from [25]. (e–f) Multimaterial option with wood biopolymer and ABS. Adapted from [30].

$14 \pm 1.2\%$ [29]. It implies lower swelling strains and responsiveness, i.e. K_{max} curvature (Fig. 17b), due to a low interlayer bond strength that cannot transfer load properly. Hygroscopic strains are the driving force behind the responsiveness of hygromorph materials and must therefore be maximized. Higher porosity leads to faster water uptake with faster actuation illustrated by a higher dK/dt ratio (Fig. 17b). dK/dt is the derivative of the curvature vs. time plot that describes the reactivity of the sample to a stimulus. Moisture diffusion and the relationship between microstructure and diffusion are the key to rapid actuation. Rapid actuation with a porous structure and high responsiveness seem paradoxical if the porosity is not optimally located in the material; a solution can be found in nature by taking inspiration from biological hydraulic actuators that have a structurally “programmed”, passive nastic actuation, such as pine cone [168,182], wheat awn [170], wild carrot

[185]. Moisture transport in biological materials is enhanced by hierarchically porous structures with nanopores in the cell wall that trigger a capillary effect [186]. Therefore, the control of the dispersion of porosity, size, and volume may be essential to control the responsiveness of the hygromorph actuator [187]. Porous structures should be built in such a way that pore networks are considered to be moisture pathways rather than mechanical defects [15]. For example, Van Opdenbosch et al. [186] have proposed that pores have strongly anisotropic shapes and perpendicular orientations within the two layers of a bilayer, helping reinforce the difference in directional expansion. Vailati et al. [188] have successfully tested the effect of milled-in grooves on wood bilayers. As the diffusion paths are shorter along the direction of the fibres, the moisture content rate and the responsiveness are increased. This principle could be transferred to 4D printing by printing gaps between

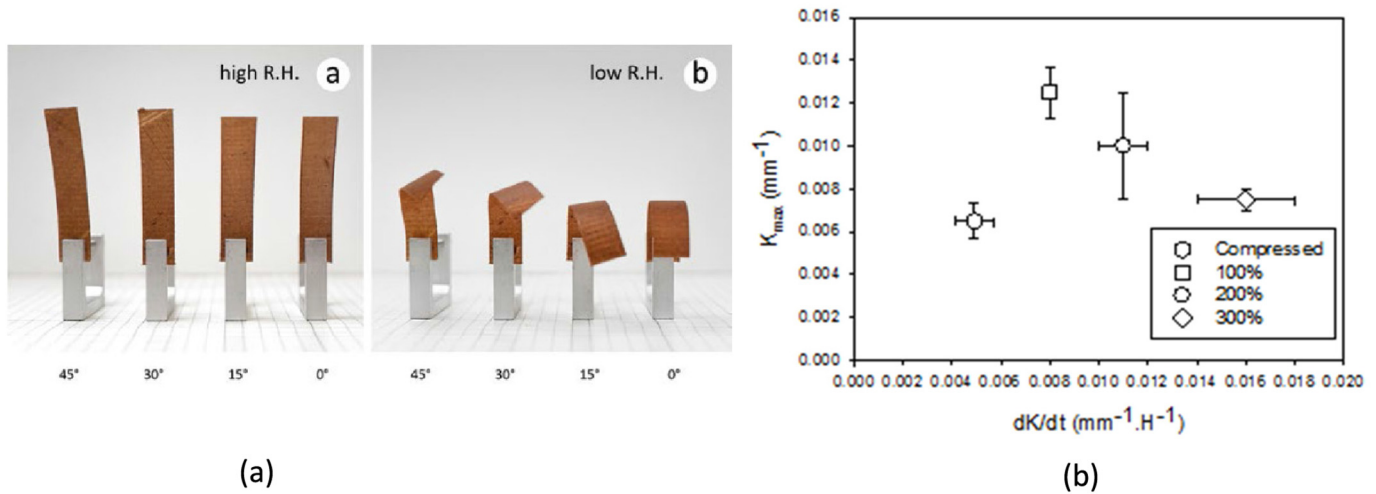


Fig. 17. (a) Effect of printing orientation on the response to different RH on the wood/biopolymer [30] and (b) Responsiveness evolution as a function of reactivity (derivative of the curvature vs. time plot) of wood/biopolymers printed in 3D for different printed configurations compared to thermocompression. (100, 200, and 300% are slicing parameters that adjust the filament width and the porosity level of the composite).

Adapted from [29] with permission of Elsevier.

several layers, which can form artificial pores, and by the strategic selection of natural fibre composites. A study from Le Duigou et al. [15] was devoted to hygromorph biocomposites manufactured by thermocompression with different natural fibres possessing different internal lumen sizes (internal porosity). Flax, jute, kenaf, and coir fibres have an internal porosity of $0.10 \pm 0.02\%$, $6.40 \pm 0.17\%$, $13.80 \pm 0.23\%$, and $39.10 \pm 0.70\%$ respectively. The higher the internal porosity, the faster the uptake of moisture, while the hygroscopic expansion is influenced by the biochemical composition of the fibres and the angle of the microfibrils. Pectin-rich fibres such as flax fibres swell faster [15], which makes them suitable candidates for future 4D printing research. Correa et al. [183] have proposed that because of the unbalanced contribution to actuation between moisture-responsive natural fibres and moisture-insensitive polymers, other stimuli should be tested to help amplify the transformation.

ii) The second strategy, also based on a bilayer architecture, is a pattern of partial filling of hygromorph biocomposites that relies on custom deposition where filament anisotropy, interfilament spacing, bonding, and surface-to-volume ratio play an important role (Fig. 16b). For example, Vazquez et al. [184] have proposed that increasing the printing path spacing from 1 to 1.5 mm, described in the literature as the road distance [170] or the distance between bead centres [189], improves both the reactivity and responsiveness of a wood/biopolymer hygromorph. Gladman et al. [25], working on cellulose/hydrogel architectures, claim that a large spacing between the filaments promotes rapid water uptake and faster actuation due to the increased surface/volume ratio. These findings could be drawn in parallel with the previous section on porous structures.

Rather than focusing on materials properties, another objective is to add a structural effect through additive manufacturing. Recent advances in digital manufacturing, i.e. the combination of additive manufacturing and numerical simulation, are needed to build complex architectures and actuation.

The second design principle concerns multimaterial printing by using a very hygroscopic material (natural fibre composite for instance) and a more or less inert polymer: ABS, PLA, Polyamide (PA) [183]. The selection of materials is made on the basis of Timoshenko's equations (Eqs. (1) and (2)) that state that an optimal curvature (responsiveness) is obtained with a higher difference of hygroscopic strains between layers, and with an optimal ratio of passive to active thickness (n ratio) depending on the tensile modulus in the two planar directions, longitudinal (L) and transversal (T) of each layer (m ratio).

Compatibility between these two materials must be checked to reduce the risk of delamination compared to monomaterials. In most cases, a dual extruder printer is used [168]. Similarly, according to the first design principle, the primary raster pattern is the hygroscopic material, where all the lines of the print path are oriented in a direction perpendicular to the desired angle of expansion. The constraint material, on the other hand, which consists of the inert polymer, is oriented parallel to the desired angle of expansion. Both types of materials could be placed locally to create an interwoven pattern (Fig. 16e) [183]. As with a pine cone scale model, the woven pattern is a matrix of multi-layer material where the main inert constraints are enclosed between the upper and lower raster layers, creating a mechanical interlock between the two layers to limit delamination of the bilayer structure [190]. Building on Timoshenko's theory, as previously established for hygroscopic bilayers [182], for both the woven pattern or the simple bonding model, the thickness of the active layer should be greater than the thickness of the constraint layer [8,172,191]. Reducing the thickness of the constraint layer coupled with increasing the porosity of the hygroscopic layer is an effective strategy to reduce the negative effect of high bending stiffness on actuation while maximizing moisture exchange and therefore responsiveness.

The use of isotropic, non-sensitive polymers creates greater differential hygroscopic swelling between the layers and, as a result, better control of actuation direction, precise angles, and response speed can be achieved. However, the use of anisotropic properties in both active and passive layers could lead to an interesting bidirectional actuation as observed in biological systems such as the pine cone scale [192,193].

Multimaterial printing combined with a localized asymmetrical structure enables to create adaptive hinges (Fig. 16f) involving a shift from curving actuation to folding [194]. The wider the width of the hinge, the smaller and faster the angle of curvature [28,30]. Today, most of the available work dedicated to hygromorph biocomposites for 4D printing is oriented towards design methodology, proof of concepts and prototypes, but information on actuation, material properties, decay, or mechanical damage remains limited.

Table 3 shows the actuation performance (reactivity and responsiveness) of different 4D printed hygromorph biocomposites based on natural fibres according to their microstructure induced by different printing strategies (full or partial monomaterial filling and multimaterials) and by external environmental conditions. Based on Timoshenko's equations, the specific actuation (actuation*thickness) for reactivity and responsiveness is presented to facilitate comparison

Table 3

Actuation properties of natural fibre-based hygromorph biocomposites (* thermocompression, ** bonded). Note: MAPP stands for Maleic Anhydride grafted PolyPropylene.

Materials and pattern		Environmental conditions	Normalized time to reach stability (h/mm)	Normalized responsiveness K.t (-)	Ref
Monomaterial copolyester-wood	Space grid	Immersion-various RH	Sorption: 5–6 Desorption: 0.10–1	0.028	[183]
	One face smooth and the other with ridges	Immersion-various RH	Sorption: 3.3–5 Desorption: 2–4	0.0285	
Monomaterial copolyester-wood	Full filling with different printing width	50%RH-immersion-50%RH	Sorption: 6.25–7.5 Desorption: 0.625	0.010	[29]
Monomaterial Cellulose/hydrogel	Space grid	Immersion in water	Sorption: <0.07	0.21–0.25	[25]
Multimaterial copolyester-wood and PA	Interwoven	Immersion-drying with heating radiation (70 °C)	Desorption: 0.021–0.0030	0.014–0.096	[183]
Multimaterial copolyester-wood and ABS	Interwoven	Relative humidity	Sorption: 12–24	0.065	
Monomaterial* MAPP/flax		50%RH-immersion-50%RH	Sorption: 3.3 Desorption: 3.3	0.037	[8,15]
Monomaterial* MAPP/flax		0–90%RH-0%RH	Sorption: 22.2 Desorption: 22	0.02	[195]
Monomaterial* MAPP/jute		50%RH-immersion-50%RH	Sorption: 5 Desorption: 4.4	0.034	[15]
Monomaterial* MAPP/kenaf		50%RH-immersion-50%RH	–	0.040	
Monomaterial* MAPP/coir		50%RH-immersion-50%RH	–	0.013	
Monomaterial** Wood		85–35%RH	Desorption: 5–10.5	0.009–0.043	[172,188,196,197]
Multimaterials* PP-PP/flax		50%RH-immersion-50%RH	Sorption: 11 Desorption: 26	0.022	[26]
Multimaterials** Wood/glass/epoxy composite		44–87%RH-44%RH	Sorption: 8.3 Desorption: 10	0.024	[191]
Multimaterials** Wood/glass/epoxy composite		44-Water sprayed-44%RH	Sorption: 3.3 Desorption: 12.5	0.0324–0.056	[174]
Multimaterials** Wood/paper		50–95%RH	x	0.0256	[176]
Multimaterials** Paper/polymer		50%RH-sprayed	x	0.032	
Multimaterials** Paper/polymer		98%RH	x	0.021	[182]

between materials. Actuation is triggered by changes in moisture content and moisture transport in the material. Most of the time, a 1D diffusion mode can be reasonably applied because of the small thickness in relation to the length and width of the samples. Where the geometry is not given in the original article, it has been estimated by image analysis. To extend the literature review, the values are compared with those of natural fibre-based hygromorph biocomposites manufactured by other processes such as thermocompression, wood bilayer glued by adhesive bonding or cellulose fibre composites. The latter should be taken with care because their operating principle is opposed to that of hygromorphic biocomposites. In composites based on cellulose fibre, the matrix swells, whereas in hygromorph biocomposites, it is the fibres that provide hygroscopic induced swelling.

The first point in evidence is the major role of the architecture of the material on the performance of the response. For monomaterials, the spacing of the filaments with space grid or ridges enhances both the responsiveness and reactivity of materials with respect to the complete filling. This is due to the maximisation of the surface exchange with moisture while reducing bending stiffness.

Regardless of the architecture, printed monomaterials evidence an asymmetrical trend in terms of actuation speed, with a faster response to desorption than to sorption. For hygromorph biocomposites based on natural fibres manufactured by thermocompression, the sorption and desorption behaviour tends to be slightly asymmetrical (Table 3). The actuation speed is not linear in time with a rapid increase for a short time and then a deceleration effect before the saturation regime is reached [29,188]. For multi-materials, the mechanisms induced by desorption tend to be slower than those occurring during sorption. This is due to the very low sensitivity of the passive layer, which may protect the active layer from air-drying by convection.

The multi-material printing method demonstrates a higher actuation responsiveness explained by the higher anisotropic ratio and the difference in swelling between layers in contrast with monomaterials. In this sense, the selection of a polymer for the passive layer with different customized thermo-hygro properties introduces a change of actuation. For example, the switch from ABS to PA results in a reverse curvature [30]. Fibre selection is also important. The type of fibres, their related microstructure in the S2 Layer (Microfibril Angle), and their biochemical composition influence the actuation of the hygromorphs. For example, coir fibres have a lower hygromorph actuation potential due to higher MFA value and a higher lignin content compared to flax and jute fibres [15]. Fibre content is a well-known parameter that influences the hygro-expansion of composites [168]. As the natural fibre content increases, hygroexpansion increases and consequently hygromorph reactivity and responsiveness. As explained in a previous section, fibre content is a crucial parameter that controls the mechanical properties of 3D printed parts. However, in the current state of technology, the fibre content is often limited due to technical concerns, as discussed earlier. Considerations regarding the high interfacial bonding ability of the fibre to the polymer and its potential impact on the hygroscopic actuation also require further investigation. This emphasizes the importance of the printing path orientation to trigger and control actuation.

The reliability of actuation with a 4D printed biocomposite hygromorph is rarely discussed in the literature in terms of the relationship between process parameters and actuation. Empirical tests on Wood/co-polyester/PA or Wood/co-polyester with a multi-material architecture subjected to a high relative humidity environment seem to show >30 actuation cycles without any significant degradation [30]. More rigorous testing has shown that the visible delamination between

the wood/co-polyester and the ABS constraint layers starts around 13 cycles [190]. Similarly, studies on monomaterials subjected to water immersion and air-drying cycles show a 50% reduction in responsiveness after the first cycle [29]. The use of multi-material assembly, i.e. Wood/co-polyester/PA, does not allow the initial properties to be retained. Correa et al. [30] have evidenced a 70% reduction in responsiveness after 4 immersion/natural drying cycles and a 50% reduction when heat radiation up to 70 °C is used for active drying.

To the best of our knowledge, no in-depth investigation has yet established the relationship between material/printing process and the reliability of actuation in a variant environment. It is worth noting that the various environmental conditions imply a wide variety of hygromorph biocomposite responses. Immersion in water results in a faster response to relative humidity due to the higher activity of the water, which leads to a faster transport of moisture and a faster expansion of the material. A similar material subjected to high relative humidity or immersion creates a difference in reactivity of a factor ranging from 2.5 on wood/composites to 5 on flax/maleic anhydride grafted polypropylene (MAPP) hygromorphs [174,191,195]. This could also be due to the change of elastic properties of the layers between these experiments [176,195].

4.3. Future trends in 4D printing of natural fibre biocomposites

In this section, an extrapolation to cellulose-based composites and hydrogel-based materials is made to open a more in-depth discussion of the potential future trends for several applications. The global 4D printing market is expected to grow at USD ~162 Million by 2022, at ~39% of CAGR between 2019 and 2022 in the fields of aerospace and defence, healthcare, automotive industry, construction, clothing, and packaging [198,199]. As mentioned by Tibbitts [200], 4D printing can integrate sensing and actuation features directly into a programmed material. Thus, external electromechanical systems are not necessary. This feature would decrease the number of parts in a structure, assembly time, material and energy costs, and the number of failure-prone devices, as usually utilized in current electromechanical systems. 4D printed biocomposites offer a novel approach to using available local resources to produce tailored autonomous and self-sufficient shape-morphing structures including adaptive underwater systems for maritime engineering (e.g. artificial reefs) [15], architectural skin systems [33], shading systems and solar tracking systems for architecture [172,190] in various environments where autonomy may be a requirement but that are not limited to extreme environments (e.g. war zones) [32].

4.3.1. At the material level

The next steps in 4D printing with natural fibre composites should target materials with improved hygroscopic properties, higher anisotropy, customized stiffness, and a high bonding ability between plies. Focusing on the rigorous selection of materials and their formulation should optimise these properties. The hygroscopic properties (sorption and swelling coefficient) of biocomposites are influenced by the type of fibre involved, i.e. their microstructure (MFA) and composition. As described earlier, the use of different species of wood or coir, jute, flax or kenaf generates a dramatic effect on the potential responsiveness of the actuator [15]. Natural fibres act as an actuating agent through swelling. Therefore, hygromorph biocomposites should be developed with the highest possible volume fraction, especially when a moisture-insensitive polymer is used. A high natural fibre content promotes faster and greater swelling [168] and therefore improves both reactivity and actuator responsiveness [15]. However, a high discontinuous fibre content increases the viscosity of the mixture and thus leads to clogging or could also prevent printing. An optimal formulation including continuous natural fibres should be investigated.

Second, the selection of a moisture-sensitive polymer matrix could also promote faster actuation. From this perspective, the best candidate

may be hydrogel polymers such as those already used by Gladman et al. [25] and Mulakkal et al. [160] with cellulose fibres. However, their moderate mechanical properties against moisture may prevent their use for technical applications in outdoor environments. Selecting a moisture-sensitive thermoplastic polymer may be an alternative. As far as the thermoplastics matrix is concerned, a low melting temperature of the polymer is to be preferred, as processing reduces the thermal degradation of the natural fibres and thus helps maintain their hygroscopic expansion [201] and actuation capacity. A lower viscosity of the polymer would promote impregnation of fibres and yarns during filament processing, improve adhesion between layers during printing, and reduce the amount of overall porosity.

As with biological systems, the anisotropy and stiffness of materials and their distribution should be well controlled to generate directional and complex actuation. This could be achieved using a combination of an oriented biocomposite with controlled swelling and a non-swelling matrix, customized control of fibre orientation within the composite, and precisely designed print path strategies across multiple layers. Customized control of fibre orientation could be achieved with precision by continuous fibres or yarns [145,166,179]. In this sense, the continuous fibre composite appears to be an encouraging solution to producing a biocomposite with programmable morphing. The technical challenge should involve the production of the filaments and their printability.

Beyond moisture-induced actuation, natural fibre composites are also sensitive to temperature. Temperature can influence the moisture content sorption and diffusion within natural fibre composites. In a wet environment, an increase of temperature accelerates the drying of biocomposites while in immersion, it speeds up the water diffusion [202]. Correa et al. [30] have used heat ranging from 70 °C to 90 °C to help the drying process of wood/biopolymer materials and enhance shape transformation. This process opens the design space to thermo-hygromorph composites with a combination of multiple stimuli. Recently, Le Duigou et al. [203] have developed a 4D printed carbon fibre-reinforced PolyAmide hygromorph where the temperature rise is controlled by Joule effects. An increase in electrical stimulation leads to an augmentation of the temperature, a reduction of the moisture content, and ultimately the control of shape morphing. The concept is named electro-thermo-hygromorph or electrical pine cone and could be applied to hygromorph biocomposites with fibre modification.

4.3.2. At the structural level

Beyond the material performance, 4D printed materials could bring about complex active structures with original actuation performance. These complex structures with original properties are often composed of periodic or non-periodic cell patterns and can be referred to as metamaterials. A strict definition of a metamaterial is a material whose properties are due to both cellular architecture and chemical composition and go beyond what is found in nature by behaving in a way not found in nature [204]. For example, Gladman et al. [25] have developed a shape-changing bioinspired structure with a complex architecture, with localized interfilament spacing to develop a gradual log-curved microstructure (Fig. 16c). Localized anisotropic swelling due to precise filament placement results in a multi-curvature actuation (Fig. 16d).

Bio-inspired mechanisms such as a multi-stage double curvature following the pine cone [27], the edge growth-driven opening of the lily flower, snap-through elastic instability based on the venus flytrap, or origami-like curved-folding kinematic amplification based on the carnivorous waterwheel plant [205] have been implemented using wood-based hygromorph biocomposites. The strength of the printing methodologies using biocomposites relies on their capacity to choreograph the direction of curvature based on the multi-layer difference between the dominant printing angle of each layer and its corresponding direction of hygro-expansion. Geometrical features such as shape, aspect ratio, or a rigid boundary can be further integrated to manipulate strain gradients across the sample [205]. For example, for one bending curvature, all the expansion due to the anisotropic orientation of the

fibre is directed along one axis. In order to obtain a double curvature (Fig. 18a and b), a specific printing pattern with a paraboloid distribution of filament is printed (Fig. 18b). The wood composite material is printed at 90° from the main axis to the centre of the specimen and the angle changes to 10° for the lateral section (Fig. 18b).

Turcaud et al. [181] have developed the concepts of “benders” or “twisters”, i.e. hygroscopic architected materials produced by monitoring the symmetry and distribution of swellable materials in their undeformed geometry. Fig. 18a presents an extrudable cross-section with different actuation patterns provided by the simulation with active and passive material distribution. Fig. 19b shows the effect of material distribution on the control of the actuation of a slender beam.

Another example of localized actuation is observed through the development of a hinge effect. Using a bilayer microstructure with multimaterial printing (nylon and wood biocomposites) on a dedicated area with a constant thickness ratio ($t_p/t_a = 1/5$) and various widths (9.5–27 mm) makes it possible to amplify the responsiveness from 98 to 161° due to a higher bending moment [30]. Unlike free displacement, the use of a hygromorph biocomposite as a hinge requires being specifically designed with appropriate stiffness and strength to generate a bending moment that lifts adjacent passive layers. As with a hinge, a fold strategy can be used. Hygromorph biocomposites can also be used to trigger actuation in a polymer system with curved crease (Fig. 20a).

Origami-type structures could be used to amplify the displacement. In addition, recent work by Baker et al. [161] on the polyurethane hydrogel/elastomer trilayer has defined the hinge zone as a “mountain” or “valley”, paving the way for origami-inspired shape-changing structures (Fig. 20b and c).

The wood/paper bilayers are assembled into a single unit cell (Fig. 21a), and then each unit cell is assembled into a honeycomb structure (Fig. 21b). There is a 20–30% difference in responsiveness between a simple bilayer and the same bilayer integrated into an alveolar structure due to geometric constraints. It is worth noting that the small strain within the active layer is converted into a large displacement ($\approx 500\%$) of the structure (Fig. 21b).

Similarly, kirigami geometries have also been tested to amplify 3D-printed multi-material structures [189]. Multi-material 3D printing is used with the inclusion of swellable polyvinyl in rigid polyurethane cell wall resins (Fig. 21a). The isotropic volume change of the highly swellable material induced by the solvent isopropanol leads to an

anisotropic volume change (+50%) of the custom-designed cell (Fig. 22a). The periodic hierarchical microstructure allows the anisotropic deformation of individual cells, resulting in unidirectional expansion/contraction of the cell structure (Fig. 22b). The thickness of the cell wall, the rigidity ratio between the cell wall and the inclusion and topology modulate the responsiveness [207].

5. Conclusion

Due to environmental and economic considerations, natural fibre-reinforced composites have been the subject of growing research interest for about 20 years, which is however a short period of time when compared to research on synthetic composites (e.g. glass or carbon fibre-reinforced composites). Despite the 20-year period, the development of biocomposites is still in its infancy in terms of technological maturity but also in terms of basic understanding. The advent of 3D and 4D printing represents a great opportunity for biocomposites to develop for the first time on the same time scale as their synthetic counterparts.

This article aimed to provide a baseline regarding the specificities of natural fibres to bolster the analysis of the mechanical and actuation properties of 3D and 4D printed biocomposites. To this end, an exhaustive literature review focusing on the printing process/microstructure and properties of natural fibre biocomposites has been achieved. Comparison has been made with synthetic materials and conventionally manufactured biocomposites. The main technical and scientific issues have been described and discussed, and new trends have been identified.

Biocomposites are used for 3D printing mainly in the form of discontinuous fibres or powder-like reinforced polymer. The current tensile properties are moderate compared to those of an established process such as injection or compression moulding. In general, it has been observed that adding natural fibres improves the stiffness of the composite but does not improve its tensile strength. 3D printed biocomposites often have a low fibre content (<30 wt%) with a very low aspect ratio (L/d) to reduce the overall viscosity and to improve printability, which accounts for their moderate properties. In addition, discontinuous or short fibre-reinforced biocomposites exhibit a high porosity content due to i) the porosity within the filament prior printing and ii) the low pressure applied during printing. This porosity induces printed samples that are likely to absorb a large amount of water, which may reduce their lifetime in a humid environment.

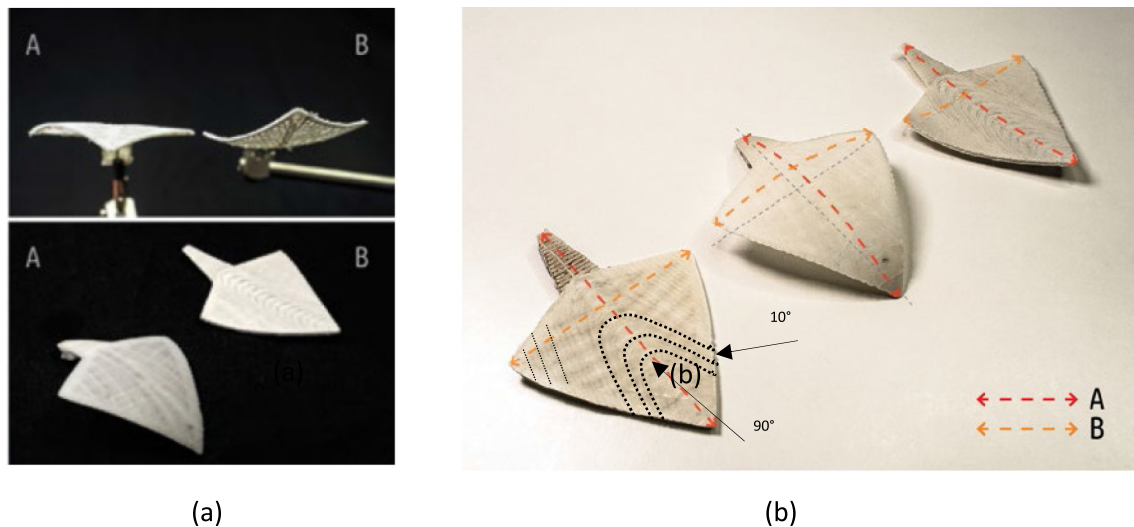


Fig. 18. (a) Three viewing perspectives of wood fibre/Biopolymer composite-responsive flap under various RH showing longitudinal and transverse curvature. (b) Example of a localized print path within the sample to induce a double curvature and multistep actuation. Adapted from [27].

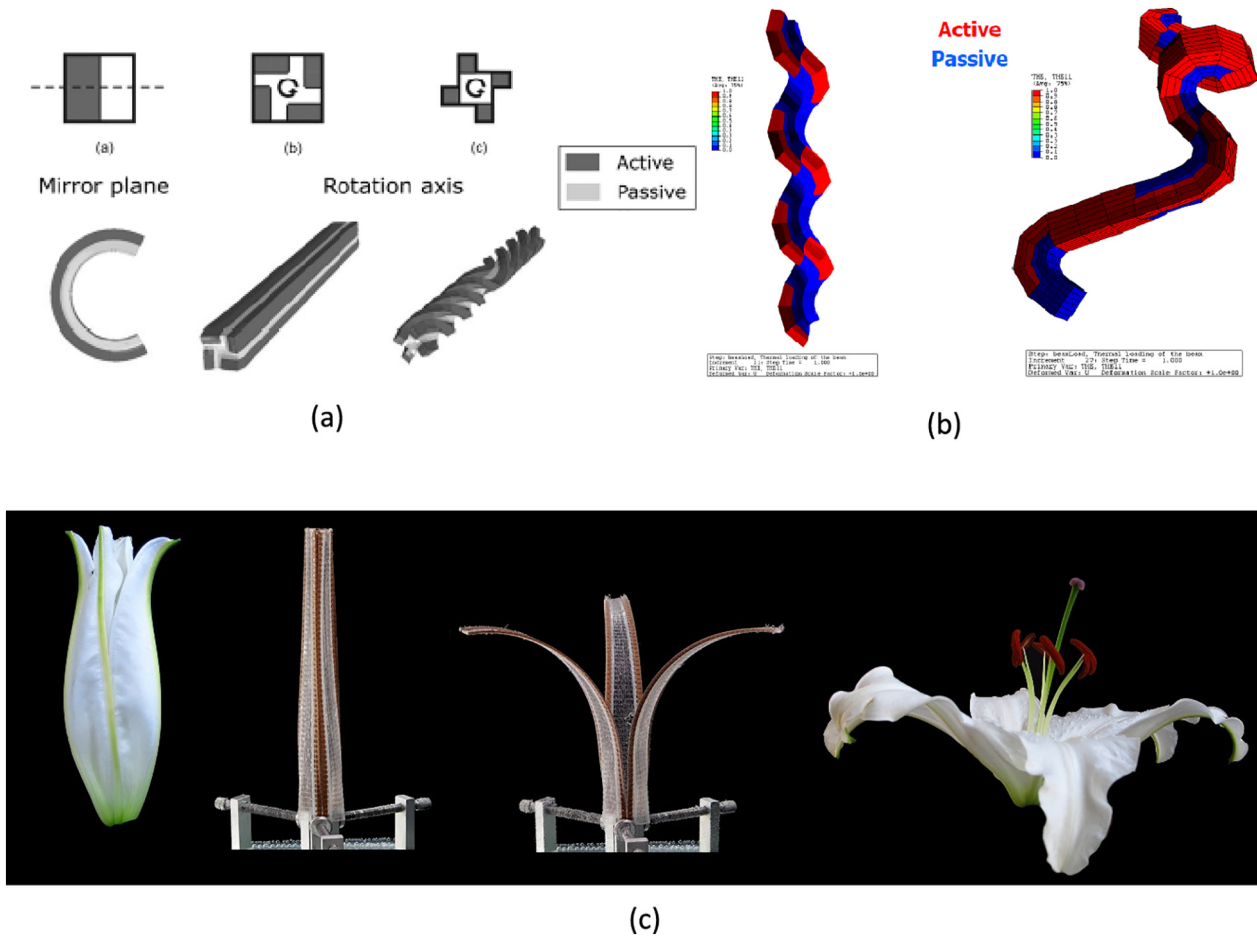


Fig. 19. (a) Simulated actuation patterns for several cross-sections with a passive/active area ratio of 50:50. Adapted from [181] Copyright© (2010) Carl Hanser Verlag GmbH & Co.KG, Muenchen. (b) Helical bending obtained by rotating the bending plane along the rod as a result of the distribution of passive (green) and active (white) regions. Adapted from [206]. (c) Edge growth causing a strain gradient in the Lilium 'Casa Blanca' drives the flower opening mechanism, a principle that is translated into a 4D printed mechanism with a wood-based hygromorph composite edge. Adapted from [205].

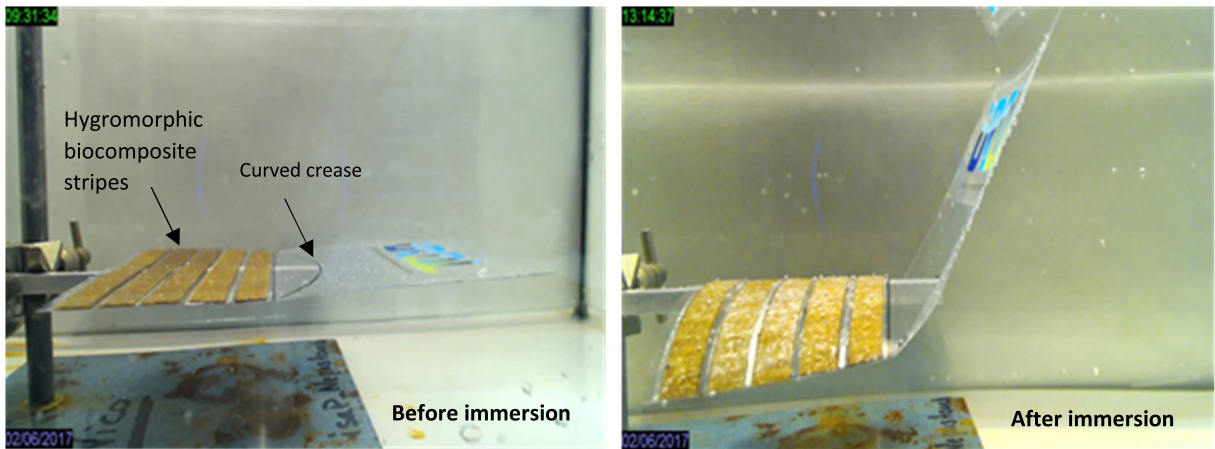
It is worth noting that synthetic counterparts such as discontinuous glass or carbon fibre-reinforced composites suffer from similar technical limitations (low fibre content and aspect ratio, high porosity content) with overall moderate properties compared to similar specimens prepared by conventional processes.

Future trends in 3D printing are expected to relate to higher mechanical properties with improved material selection. Thus, continuous natural fibre biocomposites offer a relevant alternative to discontinuous biocomposites, bringing drastically higher mechanical performance due to the higher fibre content and better control of anisotropy by fibre orientation. For this purpose, high quality natural fibre yarns (in terms of fibre variety, low twist, and low linear weight) should be industrially available in the market, and filament production with high fibre content should be investigated. The evolution of printer desktops through a controlled environment (T and RH) and customized feeding and nozzle are essential to take benefit of the full potential of natural fibres (e.g. moisture sensitivity, surface topology, tensile properties). The current machines (e.g. Markforged printers) that are able to print continuous fibre composites cannot use other materials than those they have supplied. In the near future, full characterization of the effect of printing and slicing parameters on the properties and the geometrical limitations is expected so that reliable predictive models may be developed. Complex architected composite structures, supported by disruptive design tools such as biomimicry and topological optimization, are intended

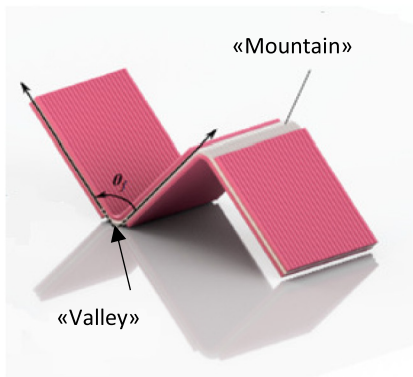
to support the development of advanced metamaterials with an enhanced and original performance.

The implementation of printing methods using 6-axis industrial robot-arm extrusion effectors is designed to facilitate the development of larger components with novel multi-axis trajectories. Moreover, the larger payload capacity of industrial manipulators is likely to facilitate the development of integrated fibre placement (both continuous and discontinuous fibres) and specialized extrusion effectors or to open the spectrum for a more diverse range of multi-material printing processes. The challenges of this development involve the issue of cost, as the material and equipment is likely to be more expensive, and complementary specifications to the Advanced Function Presentation (AFP) such as the ability of to place the tape with a low curvature (steering effect).

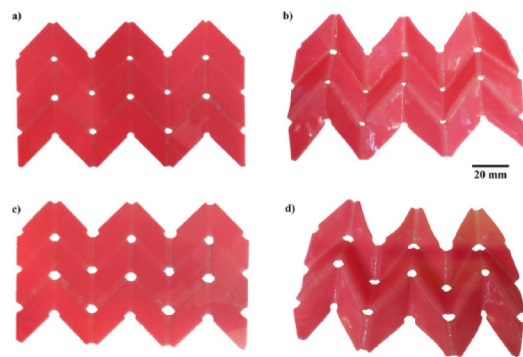
As natural fibre biocomposites have been proven to be a new class of smart materials, namely hygromorph biocomposites, they can be used in 4D printing to develop specialized shape-changing mechanisms and structures. These biocomposites, owing to their bilayer microstructure inspired by biological hydraulic actuators (e.g. pine cone), can actuate with a change in humidity or with a combination of temperature/moisture stimuli. Additive manufacturing via 4D printing is a great opportunity for hygromorph biocomposites because it facilitates the design of complex material architectures through precise manipulation of fibre orientation and distribution. Different material and design strategies using monomaterials and multimaterials can amplify the difference in



(a)

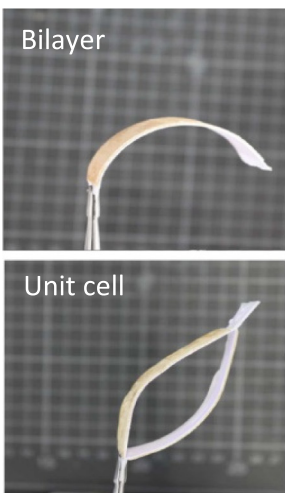


(b)

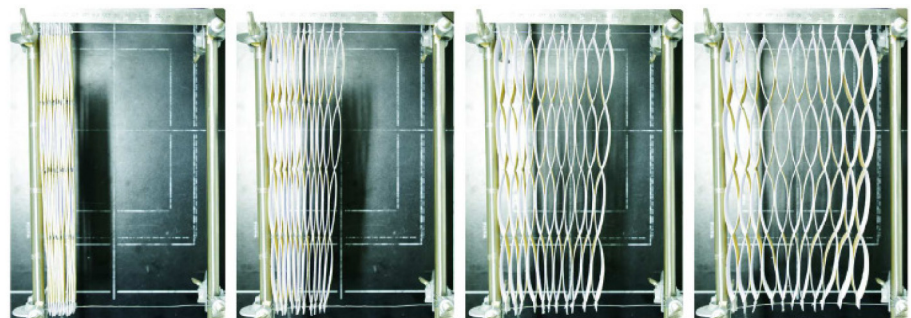


(c)

Fig. 20. (a) Moisture-induced deployable structure based on curved-line folding inspired from *aldrovanda*, adapted from [15] (b) Polyurethane hydrogel/elastomer trilayer upon dehydration showing mountain and valley folding pattern and (c) Actuation of Miura-ori origami fold pattern with the same trilayer. Adapted from [161].



(a)



(b)

Fig. 21. (a) Actuated Wood/paper bilayer and single unit cell, (b) actuation of the metamaterial made by bilayer unit cell from 0, 2, 4 and 16 h at 95% RH. Adapted from [176].

hygroexpansion between the layers. However, significant challenges remain for these technologies to develop fully. For instance, actuation performance (responsiveness and reactivity) remains slightly lower than

with conventional manufacturing due to a lower fibre content. This is a critical dimension for further research since fibres act as the main actuating agent.

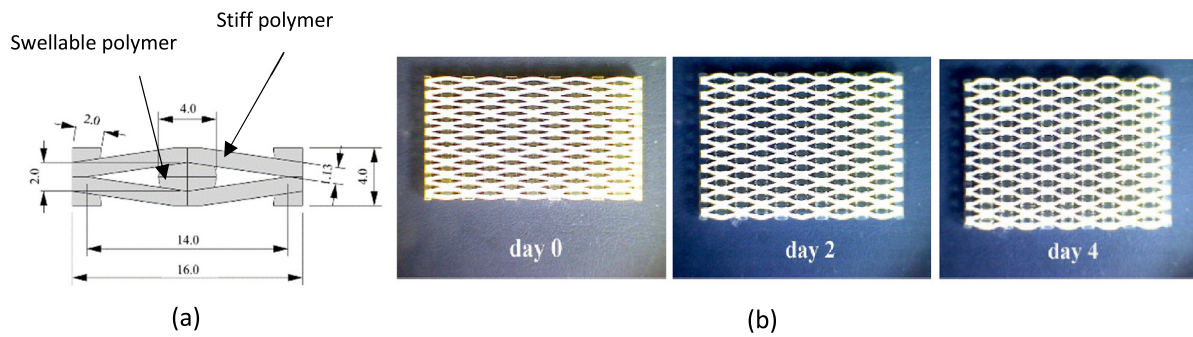


Fig. 22. (a) Schematic view of a diamond shaped unit cell inspired by the microstructure of the ice plant keel's tissue with a width-to-height ratio of 4 for stiff walls (1.13 mm thickness) and round soft inclusions. All dimensions are in mm. (b) Swelling of a honeycomb made with repetition of the diamond unit cell. The honeycombs were printed as rectangular arrays of 5-by-10 cells with stiff walls (verowhite) and soft (Tangoplus) inclusion. Snapshots cover 4 days of swelling in isopropanol at room temperature ($T = 22\text{ }^{\circ}\text{C}$). (LH-W = 50.5:5) Adapted from [176].

Further challenges exist regarding the material availability and the actuation performance and durability of the 4D printed structures. As with 3D printing, significant advances should be made regarding the quality of the materials through filament development with a wide range of polymers and fibres. The quality and the control of the microstructure are crucial to control actuation, and adapted printers must be proposed. For actuation of the morphing performance, the future trends could occur on two levels: material and structure. At the material level, the aim is to produce biocomposites with enhanced hydroexpansion (kinetic and amplitude) but durable against degradation. In addition, passive stimulus response could be combined with active electromechanical systems to enhance multifunctionality and the range of applications.

At the structure level, the target is to geometrically amplify the actuation of the unit cells by designing metamaterials. Thus, hygromorph biocomposites will be used as a building element towards a more complex structure whose morphing properties depend on both the material and geometric considerations. Finally, the most exciting challenge in the field of the 3D/4D printing of natural fibre biocomposites is probably to overcome the current material design habits by developing real multi-disciplinary work involving eco-design, biomimicry, mechanics, materials sciences, technology, and other disciplines.

CRediT authorship contribution statement

Antoine Le Duigou: Conceptualization, Investigation, Funding acquisition, Methodology, Project administration, Supervision, Validation, Visualization, Writing - original draft, Writing - review & editing. **David Correa:** Conceptualization, Writing - review & editing. **Masahito Ueda:** Writing - review & editing. **Ryosuke Matsuzaki:** Writing - review & editing. **Mickaël Castro:** Conceptualization, Writing - review & editing.

Declaration of Competing Interest

The authors declare that they have no known competing financial interests or personal relationships that could have appeared to influence the work reported in this paper.

Acknowledgements

The authors are grateful to the CNRS AAP "Biomimétisme" for its financial support and Nicole Geslin for post-editing the English style.

Data availability

The raw/processed data needed to replicate these results cannot be shared at this time as they are part of an ongoing study.

References

- [1] J. Dizon, A. Espera Jr., Q. Chen, R. Advincula, Mechanical characterization of 3D-printed polymers, *Addit Manuf* 20 (2018) 44–67.
- [2] T. Ngo, A. Kashani, G. Imbalzano, K. Nguyen, D. Hui, Additive manufacturing (3D printing): a review of materials, methods, applications and challenges, *Compos. Part B* 143 (2018) 172–196, <https://doi.org/10.1016/j.compositesb.2018.02.012>.
- [3] A. Mitchell, U. Lafont, M. Holyńska, C. Semprinoschnig, Additive manufacturing - a review of 4D printing and future applications, *Addit Manuf* 24 (2018) 606–626.
- [4] S. Kabir, K. Mathur, A. Seyam, A critical review on 3D printed continuous fiber-reinforced composites: history, mechanism, materials and properties, *Compos. Struct.* (2019) <https://doi.org/10.1016/j.compstruct.2019.111476>.
- [5] L.G. Blok, M.L. Longana, H. Yu, B.K.S. Woods, An investigation into 3D printing of fibre reinforced thermoplastic composites, *Addit Manuf* 22 (2018) 176–186, <https://doi.org/10.1016/j.addma.2018.04.039>.
- [6] A. Woern, J. Pearce, Distributed manufacturing of flexible products: technical feasibility and economic viability, *Technologies* 5 (2017) 71, <https://doi.org/10.3390/technologies5040071>.
- [7] P. Parandoush, D. Lin, Review on additive manufacturing of polymer-fiber composites, *Compos. Struct.* 182 (2017) 36–53.
- [8] A. Le Duigou, M. Castro, Hygromorph bio composites: effect of fibre content and interfacial strength on the actuation performances, *Ind. Crop. Prod.* 99 (2017) <https://doi.org/10.1016/j.indcrop.2017.02.004>.
- [9] D. Cole, J. Riddick, H. Jaim, K. Strawhecker, N. Zander, Interfacial mechanical behavior of 3D printed ABS, *J. Appl. Polym. Sci.* 133 (2016) 913, <https://doi.org/10.1002/app.43671>.
- [10] F. Brites, C. Malça, F. Gaspar, J. Horat, M. Franco, S. Biscaia, et al., Cork plastic composite optimization for 3D printing applications, *Procedia Manuf* 12 (2017) 156–165.
- [11] X. Wang, M. Jiang, Z. Zhou, J.H.D. Gou, 3D printing of polymer matrix composites: a review and prospective, *Compos Part B Eng* 110 (2017) 442–458.
- [12] Z. Khoo, J. Teoh, Y. Liu, C. Chua, S. Yang, J. An, et al., 3D printing of smart materials: a review on recent progresses in 4D printing, *Virtual Phys Prototyp* 10 (2015) 103–122.
- [13] A. Boumaud, J. Beaugrand, D. Shah, V. Placet, C. Baley, Towards the design of high performance biocomposites, *Prog. Mater. Sci.* 97 (2018) 347–408.
- [14] V. Sekar, M. Fouladi, S. Namasivayam, S. Sivakumar, Additive manufacturing: a novel method for developing an acoustic panel made of natural fiber-reinforced composites with enhanced mechanical and acoustical properties, *J Eng* (2019) 1–19.
- [15] A. Le Duigou, S. Requile, J. Beaugrand, F. Scarpa, M. Castro, Natural fibres actuators for smart bio-inspired hygromorph biocomposites, *Smart Mater. Struct.* 26 (2017) <https://doi.org/10.1088/1361-665X/aa9410>.
- [16] O. Faruk, A.K. Bledzki, H.-P. Fink, M. Sain, Biocomposites reinforced with natural fibers: 2000–2010, *Prog. Polym. Sci.* 37 (2012) 1552–1596, <https://doi.org/10.1016/j.progpolymsci.2012.04.003>.
- [17] C. Baley, M. Gomina, J. Beard, A. Bourmaud, S. Drapier, M. Ferreira, et al., Specific features of flax fibres used to manufacture composite materials, *Int. J. Mater. Form.* (2018) 1–30.
- [18] A. Mohanty, M. Misra, L. Drzal, Sustainable bio-composites from renewable resources, *J. Polym. Environ.* 10 (2002) 19–26.
- [19] K. Pickering, M. Aruan Efendy, T. Le, A review of recent developments in natural fibre composites and their mechanical performance, *Compos Part A Appl Sci Manuf* 83 (2015) 98–112, <https://doi.org/10.1016/j.compositesa.2015.08.038>.
- [20] N. de Bruyne, Plastic progress - some further developments in the manufacture and use of synthetic materials for aircraft construction, *Flight* (1939) 77–79.
- [21] S. Tibbitts, The emergence of 4D printing, TED Talks, 2013.
- [22] Q. Ge, H.J. Qi, M.L. Dunn, Active materials by four-dimension printing, *Appl. Phys. Lett.* 103 (2013) <https://doi.org/10.1063/1.4819837>.
- [23] E. Pei, 4D printing: dawn of an emerging technology cycle, *Assem. Autom.* 34 (2014) 310–314, <https://doi.org/10.1108/AA-07-2014-062>.

- [24] S. Miao, N. Castro, M. Nowicki, L. Xia, H. Cui, X. Zhou, et al., 4D printing of polymeric materials for tissue and organ regeneration, *Mater. Today* 20 (2017) 577–591, <https://doi.org/10.1016/j.mat.2017.06.005>.
- [25] S. Gladman, E. Matsumoto, R. Nuzzo, L. Mahadevan, J. Lewis, Biomimetic 4D printing, *Nat. Mater.* 15 (2016) 413–418, <https://doi.org/10.1016/j.proeng.2018.01.056>.
- [26] A. Le Duigou, M. Castro, Moisture-induced self-shaping flax-reinforced polypropylene biocomposite actuator, *Ind. Crop. Prod.* 71 (2015) <https://doi.org/10.1016/j.indcrop.2015.03.077>.
- [27] D. Correa, A. Menges, Fused filament fabrication for multi kinetic state climate responsive aperture, *Fabr Chapter 3 Rethink Addit Startegies*, UCL Press 2017, pp. 190–195, <https://doi.org/10.2307/j.ctt1n7kqk7.30>.
- [28] D. Correa, A. Menges, 3D printed hygroscopic programmable material systems, *MRS Online Proceeding Libr Arch* (2015) 1800.
- [29] A. Le Duigou, M. Castro, R. Bevan, N. Martin, 3D printing of wood fibre biocomposites: from mechanical to actuation functionality, *Mater. Des.* 97 (2016) 347–408, <https://doi.org/10.1016/j.matdes.2016.02.018>.
- [30] D. Correa, A. Papadopoulou, C. Guberan, N. Jhaveri, S. Reichert, A. Menges, et al., 3D-printed wood: programming hygroscopic material transformations, *3D Print Addit Manuf* 2 (2015) 106–116, <https://doi.org/10.1089/3dp.2015.0022>.
- [31] A. Lee, J. An, C. Chua, Two-way 4D printing: a review on the reversibility of 3D-printed shape memory materials, *Eng Mater* 3 (2017) 663–674, <https://doi.org/10.1016/j.ENG.2017.05.014>.
- [32] F. Momeni, S. Medhi Hassani, X. Liu, J. Ni, A review of 4D printing, *Mater. Des.* 122 (2017) 42–79, <https://doi.org/10.1016/j.matdes.2017.02.068>.
- [33] E. Vazquez, C. Randall, J. Duarte, Shape-changing architectural skins a review on materials, design and fabrication strategies and performance analysis, *J Facade Des Eng* 7 (2019) <https://doi.org/10.7480/jfde.2019.2.3877>.
- [34] Z. Zhang, K. Demir, G. Gu, Developments in 4D-printing: a review on current smart materials, technologies, and applications, *Int J Smart Nano Mater* 3 (2019) 1–20, <https://doi.org/10.1080/19475411.2019.1591541>.
- [35] N. Defoirdt, S. Biswas, L. De Vriese, Tran LQN, J. Van Acker, Q. Ahsan, et al., Assessment of the tensile properties of coir, bamboo and jute fibre, *Compos Part A Appl Sci Manuf* 41 (2010) 588–595, <https://doi.org/10.1016/j.compositesa.2010.01.005>.
- [36] P. Fratzi, R. Elbaum, I. Burgert, Cellulose fibrils direct plant organ movements, *Faraday Discuss.* 139 (2008) 275–282.
- [37] T. Joffe, R.C. Neagu, S.L. Bardage, E.K. Gamstedt, Modelling of the hygroelastic behaviour of normal and compression wood tracheids, *J. Struct. Biol.* 185 (2014) 89–98, <https://doi.org/10.1016/j.jsb.2013.10.014>.
- [38] A. Lefevre, A. Bourmaud, C. Morvan, C. Baley, Elementary flax fibre tensile properties: correlation between stress-strain behaviour and fibre composition, *Ind. Crop. Prod.* 52 (2014) 762–769, <https://doi.org/10.1016/j.indcrop.2013.11.043>.
- [39] A. Le Duigou, A. Bourmaud, E. Balnois, P. Davies, C. Baley, Improving the interfacial properties between flax fibres and PLLA by a water fibre treatment and drying cycle, *Ind. Crop. Prod.* 39 (2012) 31–39, <https://doi.org/10.1016/j.indcrop.2012.02.001>.
- [40] C. Baley, Y. Perrot, F. Busnel, H. Guezenoc, P. Davies, Transverse tensile behaviour of unidirectional plies reinforced with flax fibres, *Mater. Lett.* 60 (2006) 2984–2987, <https://doi.org/10.1016/j.matlet.2006.02.028>.
- [41] C. Baley, Analysis of the flax fibres tensile behaviour and analysis of the tensile stiffness increase, *Compos Part A Appl Sci Manuf* 33 (2002) 939–948, [https://doi.org/10.1016/S1359-835X\(02\)00040-4](https://doi.org/10.1016/S1359-835X(02)00040-4).
- [42] V. Placet, O. Cissé, M. Lamine Boubakar, Nonlinear tensile behaviour of elementary hemp fibres. Part I: investigation of the possible origins using repeated progressive loading with in situ microscopic observations, *Compos Part A Appl Sci Manuf* 56 (2014) 319–327, <https://doi.org/10.1016/j.compositesa.2012.11.019>.
- [43] D. Shah, Damage in biocomposites: stiffness evolution of aligned plant fibre composites during monotonic and cyclic fatigue loading, *Compos Part A Appl Sci Manuf* (2015) <https://doi.org/10.1016/j.compositesa.2015.09.008>.
- [44] N. Martin, N. Mouret, P. Davies, C. Baley, Influence of the degree of retting of flax fibers on the tensile properties of single fibers and short fiber/polypropylene composites, *Ind. Crop. Prod.* 49 (2013) 755–767, <https://doi.org/10.1016/j.indcrop.2013.06.012>.
- [45] A. Bismarck, I. Aranberri-Askargorta, J. Springer, T. Lampke, B. Wielage, A. Stamboulis, et al., Surface characterization of flax, hemp and cellulose fibers: surface properties and the water uptake behavior, *Polym. Compos.* 23 (2002) 872–894.
- [46] A. Gallos, G. Paes, F. Allais, J. Beaugrand, Lignocellulosic fibers: a critical review of extrusion process for enhancement of the properties of natural fiber composites, *R Soc Chem* 7 (2017).
- [47] A. Le Duigou, A. Kervoelen, A. Le Grand, M. Nardin, C. Baley, Interfacial properties of flax fibre-epoxy resin systems: existence of a complex interphase, *Compos. Sci. Technol.* 100 (2014) <https://doi.org/10.1016/j.compscitech.2014.06.009>.
- [48] N. Le Moigne, M. Longerey, J. Taulemesse, J. Bénétet, A. Bergeret, Study of the interface in natural fibres reinforced poly (lactic acid) biocomposites modified by optimized organosilane treatments, *Ind. Crop. Prod.* 52 (2014) 481–494.
- [49] A. Le Duigou, C. Baley, Y. Grohens, P. Davies, J.-Y. Cognard, R. Créach/Cadec, et al., A multi-scale study of the interface between natural fibres and a biopolymer, *Compos Part A Appl Sci Manuf* 65 (2014) <https://doi.org/10.1016/j.compositesa.2014.06.010>.
- [50] A. Bourmaud, C. Morvan, A. Bouali, V. Placet, P. Perré, C. Baley, Relationships between micro-fibrillar angle, mechanical properties and biochemical composition of flax fibers, *Ind. Crop. Prod.* 44 (2013) <https://doi.org/10.1016/j.indcrop.2012.11.031>.
- [51] O. Arnould, D. Siniscalco, A. Bourmaud, A. Le Duigou, C. Baley, Better insight into the nano-mechanical properties of flax fibre cell walls, *Ind. Crop. Prod.* 97 (2017) 224–228, <https://doi.org/10.1016/j.indcrop.2016.12.020>.
- [52] C. Morvan, C. Andème-Onzighi, R. Girault, D.S. Himmelsbach, A. Driouch, D.E. Akin, Building flax fibres: more than one brick in the walls, *Plant Physiol. Biochem.* 41 (2003) 935–944, <https://doi.org/10.1016/j.plaphy.2003.07.001>.
- [53] J. Beaugrand, F. Berzin, Lignocellulosic fiber reinforced composites: influence of compounding conditions on defibrization and mechanical properties, *J. Appl. Polym. Sci.* 128 (2013) 1227–1238.
- [54] A. Le Duigou, I. Pillin, A. Bourmaud, P. Davies, C. Baley, Effect of recycling on mechanical behaviour of biocompostable flax/poly (L-lactide) composites, *Compos Part A Appl Sci Manuf* 39 (2008) 1471–1478, <https://doi.org/10.1016/j.compositesa.2008.05.008>.
- [55] B. Madsen, A. Thygesen, H. Lilholt, Plant fibre composites – porosity and volumetric interaction, *Compos. Sci. Technol.* 67 (2007) 1584–1600, <https://doi.org/10.1016/j.compscitech.2006.07.009>.
- [56] G. Coroller, A. Lefevre, A. Le Duigou, A. Bourmaud, G. Ausias, T. Gaudry, et al., Effect of flax fibres individualisation on tensile failure of flax/epoxy unidirectional composite, *Compos Part A Appl Sci Manuf* 51 (2013) 62–70, <https://doi.org/10.1016/j.compositesa.2013.03.018>.
- [57] A. Kelly, W.R. Tyson, Tensile properties of fibre-reinforced metals: copper/tungsten and copper/molybdenum, *J Mech Phys Solids* 13 (1965) 329–350, [https://doi.org/10.1016/0022-5096\(65\)90035-9](https://doi.org/10.1016/0022-5096(65)90035-9).
- [58] C. Badouard, F. Traon, C. Denoual, C. Mayer-Laigle, G. Paës, A. Bourmaud, Exploring mechanical properties of fully compostable flax reinforced composite filaments for 3D printing applications, *Ind. Crop. Prod.* 135 (2019) 246–250.
- [59] A. Lefevre, A. Le Duigou, A. Bourmaud, A. Kervoelen, C. Morvan, C. Baley, Analysis of the role of the main constitutive polysaccharides in the flax fibre mechanical behaviour, *Ind. Crop. Prod.* 76 (2015) 1039–1048, <https://doi.org/10.1016/j.indcrop.2015.07.062>.
- [60] C.A.S. Hill, A. Norton, G. Newman, The water vapor sorption behavior of natural fibers, *J. Appl. Polym. Sci.* 112 (2009) 1524–1537, <https://doi.org/10.1002/app.29725>.
- [61] A. Bismarck, S. Mishra, T. Lampke, A.K. Mohanty, M.D.L. Mishra, Plant fibers as reinforcement for green composites, *Nat. Fibers, Biopolym Biocomposites*, CRC Press, Boca Rat, 2005.
- [62] K. Pickering, Properties and Performance of Natural-fibre Composites, 1st ed Woodhead Publ, 2008 576.
- [63] A. Monti, E. Alexopoulou (Eds.), *Kenaf: A Multi-Purpose Crop for Several Industrial Applications*, Springer London, London, 2013.
- [64] A.K. Bledzki, J. Gassan, Composites reinforced with cellulose based fibres, *Prog. Polym. Sci.* 24 (1999) 221–274.
- [65] N. Dayakar, Effective Properties of Randomly Oriented Kenaf Short Fiber Reinforced, by Dayakar Naik L. Thesis Rep Utah State University, 2015 <https://digitalcommons.usu.edu/cgi/viewcontent.cgi?article=5599&context=etd>.
- [66] H.M. Akil, M.F. Omar, A. Mazuki, S. Safiee, Z. Ishak, A. Abu Bakar, Kenaf fiber reinforced composites: a review, *Mater. Des.* 32 (2011) 4107–4121, <https://doi.org/10.1016/j.matdes.2011.04.008>.
- [67] R. Mahjoub, J. Yatim, A. Sam, S. Hashemi, Tensile properties of kenaf fiber due to various conditions of chemical fiber surface modifications, *Constr. Build. Mater.* 55 (2014) 103–113.
- [68] A. Bourmaud, A. Le Duigou, C. Baley, Mechanical Performance of Flax-based Biocomposites, 2015 <https://doi.org/10.1016/B978-1-78242-373-7.00013-5>.
- [69] A. Komuriah, N. Kumar, B. Prasad, Chemical composition of natural fibers and its influence on their mechanical properties, *Mech. Compos. Mater.* 50 (2014).
- [70] M. Eder, O. Arnould, J. Dunlop, J. Hornatowska, L. Salmen, Experimental micromechanical characterisation of wood cell walls, *Wood Sci. Technol.* 43 (2013).
- [71] L. Marrot, A. Lefevre, B. Pontoire, A. Bourmaud, C. Baley, Analysis of the hemp fiber mechanical properties and their scattering (Fedora 17), *Ind. Crop. Prod.* 51 (2013) 317–327, <https://doi.org/10.1016/j.indcrop.2013.09.026>.
- [72] V. Placet, O. Cisse, M.L. Boubakar, Influence of environmental relative humidity on the tensile and rotational behaviour of hemp fibres, *J. Mater. Sci.* 47 (2011) 3435–3446, <https://doi.org/10.1007/s10853-011-6191-3>.
- [73] S. Eichhorn, R. Young, Composite micromechanics of hemp fibres and epoxy resin microdroplets, *Compos. Sci. Technol.* (2004) 767–772.
- [74] M. Kariz, M. Sernek, M. Obućina, M. Kuzman, Effect of wood content in FDM filament on properties of 3D printed parts, *Mater. Today* 14 (2017) 135–140.
- [75] D. Stoof, K. Pickering, Y. Zhang, Fused deposition modeling of natural fibre/polylactic acid composites, *J Compos Sci* 1 (2017) 8.
- [76] G. Xie, Y. Zhang, W. Lin, Plasticizer combinations and performance of wood flour-poly (lactic acid) 3D printing filaments, *Bio Resources* 12 (2017) 6736–6748, <https://doi.org/10.15376/biores.12.3.6736-6748>.
- [77] A.R. Torrado Perez, D.A. Roberson, R.B. Wicker, Fracture surface analysis of 3D printed tensile specimens of novel ABS based materials, *J Fail Anal Preven* 14 (2014) 343–353.
- [78] D. Stoof, K. Pickering, Sustainable composite fused deposition modeling filament using recycled pre-consumer polypropylene, *Compos Part B Eng* 135 (2018) 110–118.
- [79] D. Filgueira, S. Holmen, J. Melbø, D. Moldes, A. Echtermeyer, G. Chinga-Carrasco, 3D printable filaments made of biobased polyethylene biocomposites, *Polymers (Basel)* 10 (2018) 314, <https://doi.org/10.3390/polym10030314>.
- [80] T.N. Tran, I.S. Bayer, J.A. Heredia-Guerrero, M. Frugone, M. Lagomarsino, F. Maggio, et al., Cocoa shell waste biofilaments for 3D printing applications, *Macromol. Mater. Eng.* (2017) <https://doi.org/10.1002/mame.201700219>.
- [81] H. Bi, Z. Ren, R. Guo, M. Xu, Y. Song, Fabrication of flexible wood flour/thermoplastic polyurethane elastomer composites using fused deposition molding, *Ind. Crop. Prod.* 122 (2018) 76–84.

- [82] F. Cichocki Jr., J. Thomason, Thermoelastic anisotropy of a natural fiber, *Compos. Sci. Technol.* 62 (2002) 669–678, [https://doi.org/10.1016/S0266-3538\(02\)00011-8](https://doi.org/10.1016/S0266-3538(02)00011-8).
- [83] C. Baley, A. Le Duigou, A. Bourmaud, P. Davies, Influence of drying on the mechanical behaviour of flax fibres and their unidirectional composites, *Compos Part A Appl Sci Manuf* 43 (2012) 1226–1233, <https://doi.org/10.1016/j.compositesa.2012.03.005>.
- [84] T. Yang, Effect of extrusion temperature on the physico-mechanical properties of unidirectional wood fiber reinforced polylactic acid composite (WFRPC) components using fused deposition modeling, *Polymers (Basel)* 10 (2018) 1–11.
- [85] M. Pucci, P. Liotier, D. Seveno, C. Fuentes, A.W. Van Vuure, S. Drapier, Swelling of flax fibres: effect of thermal treatment on their dimensional stability, *ECCM 17*, 2016, (26–30 June).
- [86] P. Gérardin, M. Petric, M. Petrisans, J. Lambert, J.J. Ehrhardt, Evolution of wood surface free energy after heat treatment, *Polym Degrad Stab* 92 (2007) 653–657.
- [87] P. Parlevliet, H. Bersee, A. Beukers, Residual stresses in thermoplastic composites—a study of the literature—part I: formation of residual stresses, *Comp Part A Appl Sci Manuf* 37 (2006) 1847–1857.
- [88] P. Parlevliet, H. Bersee, A. Beukers, Residual stresses in thermoplastic composites—a study of the literature—part II: experimental techniques, *Comp Part A Appl Sci Manuf* 38 (2007) 651–655.
- [89] W. Zhang, A. Wu, J. Sun, Z. Quan, B. Gu, B. Sun, et al., Characterization of residual stress and deformation in additively manufactured ABS polymer and composite specimens, *Compos. Sci. Technol.* 150 (2017) 102–110.
- [90] X. Xiao, V. Chevali, P. Song, D. Hed, H. Wang, Polylactide/hemp hurd biocomposites as sustainable 3D printing feedstock, *Compos. Sci. Technol.* (2019) <https://doi.org/10.1016/j.compscitech.2019.107887>.
- [91] J. Thomason, Why natural fibres failing to deliver on composite performance? *Int Conf Compos Mater ICCM17 Proc*, 2009, doi <http://www.iccm-central.org/Proceedings/ICCM17proceedings/Themes/Materials/NATURAL%20FIBRE%20COMPOSITES/D9.1%20Thomason.pdf>.
- [92] F. Gentles, J. Anderson, J.L. Thomason, Characterisation of the transverse thermoelastic properties of natural fibres used in composites, 14th Eur. Conf. Compos. Mater. ECCM14, 7–10 June 2010, Budapest, 2010.
- [93] J. Thomason, Dependence of interfacial strength on the anisotropic fiber properties of jute reinforced composites, *Polym. Compos.* 31 (2009) 1525–1534.
- [94] A. le Duigou, J. Merotte, A. Bourmaud, P. Davies, K. Belhouli, C. Baley, Hygroscopic expansion: a key point to describe natural fibre/polymer matrix interface bond strength, *Compos. Sci. Technol.* 151 (2017) <https://doi.org/10.1016/j.compscitech.2017.08.028>.
- [95] G. Gamona, P. Evon, L. Rigal, Twin-screw extrusion impact on natural fibre morphology and material properties in poly (lactic acid) based biocomposites, *Ind. Crop. Prod.* 46 (2013) 173–185, <https://doi.org/10.1016/j.indcrop.2013.01.026>.
- [96] B. Coppola, E. Garofalo, L. Di Maio, P. Scarfatao, L. Incarnato, Investigation on the use of PLA/hemp composites for the fused deposition modelling (FDM) 3D printing, *AIIP Conf Proc* (2018) 1981.
- [97] M. Milosevic, A. Stoof, K. Pickering, Characterizing the mechanical properties of fused deposition modeling natural fiber recycled polypropylene composites, *J Compos Sci* 1 (2017) 7.
- [98] D. Stoof, K. Pickering, Fused deposition modeling of natural fibre/polylactic acid composites, *J Compos Sci* 1 (2017) 8, <https://doi.org/10.3390/jcs1010008>.
- [99] D. Depuydt, M. Balthazar, K. Hendrickx, W. Six, E. Ferraris, F. Desplentere, et al., Production and characterization of bamboo and flax fiber reinforced polylactic acid filaments for fused deposition modeling (FDM), *Polym. Compos.* (2018) <https://doi.org/10.1002/pc.24971>.
- [100] D. Zhao, X. Cai, G. Shou, Y. Gu, P. Wang, Study on the preparation of bamboo plastic composite intend for additive manufacturing, *Key Eng. Mater.* 667 (2016) 250–258.
- [101] M. Pop, C. Croitoru, T. Bedő, V. Geamran, I. Radomir, M. Cosnita, et al., Structural changes during 3D printing of bionderived and synthetic thermoplastic materials, *J. Appl. Polym. Sci.* 47382 (2019) 1–12, <https://doi.org/10.1002/app.47382>.
- [102] M. Navarrete, I. Jorge, M. Hidalgo-Salazar, E. Escobar Nunez, A.J. Rojas Arciniegas, Thermal and mechanical behavior of biocomposites using additive manufacturing, *Int. J. Interact. Des. Manuf.* (2017) <https://doi.org/10.1007/s12008-017-0411-2>.
- [103] H. Liu, H. He, X. Peng, B. Huang, J. Li, Three-dimensional printing of poly (lactic acid) bio-based composites with sugarcane bagasse fiber: effect of printing orientation on tensile performance, *Polym. Adv. Technol.* 30 (2019) 910–922.
- [104] F. Daver, K. Peng, M. Lee, M. Brandt, R. Shanks, Cork-PLA composite filaments for fused deposition modelling, *Compos. Sci. Technol.* 168 (2018) 230–237.
- [105] J. Safka, M. Ackermann, J. Bobeck, M. Seidl, J.B.L. Habr, Use of composite materials for FDM 3D print technology, *Mater. Sci. Forum* 862 (2016) 174–181.
- [106] A. Kearns, Cotton cellulose fibers for 3D print material, Thesis Rep 2017. <https://repository.lib.ncsu.edu/bitstream/handle/1840.20/33730/etd.pdf?sequence=1&isAllowed=y>.
- [107] Y. Tao, H. Wang, Z. Li, P. Li, S.Q. Shi, Development and application of wood flour-filled polylactic acid composite filament for 3D printing, *Materials (Basel)* 10 (2017) 1–6, <https://doi.org/10.3390/ma10040339>.
- [108] Filgueira, D., Holmen, S., Melbø, J. K., Moldes, D., Echtermeyer, A. T., & Chinga-Carrasco G. Enzymatic-assisted modification of thermomechanical pulp fibers to improve the interfacial adhesion with poly (lactic acid) for 3D printing. 5(10), 9338–9346. *ACS Sustain. Chem. Eng.* 2017; 5: 9338–46.
- [109] Y. Tao, L. Pan, D. Liu, P. Li, A case study: mechanical modeling optimization of cellular structure fabricated using wood flour-filled polylactic acid composites with fused deposition modelling, *Compos. Struct.* 216 (2019) 360–365.
- [110] N. Zander, J. Park, Z. Boelter, M. Gillan, Recycled cellulose polypropylene composite feedstocks for material extrusion additive manufacturing, *ACS Omega* 4 (2019) 13879–13888.
- [111] J. Girdis, L. Gaudion, G. Proust, S. Loschke, A. Dong, Rethinking timber: investigation into the use of waste macadamia nut shells for additive manufacturing, *JOM* 69 (2017) 575–579.
- [112] A. Bourmaud, D. Åkesson, J. Beaugrand, A. Le Duigou, M. Skrifvars, C. Baley, Recycling of L-poly-(lactide)-poly-(butylene-succinate)-flax biocomposite, *Polym. Degrad. Stab.* 128 (2016) 77–88, <https://doi.org/10.1016/j.polymdegradstab.2016.03.018>.
- [113] A. Bourmaud, C. Baley, Investigations on the recycling of hemp and sisal fibre reinforced polypropylene composites, *Polym. Degrad. Stab.* 92 (2007) 1034–1045, <https://doi.org/10.1016/j.polymdegradstab.2007.02.018>.
- [114] X. Zhao, H. Tekinalp, X. Meng, D. Ker, B. Benson, Y. Pu, et al., Poplar as biofiber reinforcement in composites for large-scale 3D printing, *ACS Appl Bio Mater* (2019) <https://doi.org/10.1021/acsabm.9b00675>.
- [115] S. Kyle, Z. Jessop, A. Al-Sabah, I. Whitaker, “Printability” of candidate biomaterials for extrusion based 3D printing: state-of-the-art, *Adv Healthc Mater* (2017), 1700264, <https://doi.org/10.1002/adhm.201700264>.
- [116] M. Osman, M. Atia, Investigation of ABS-rice straw composite feedstock filament for FDM, *Rapid Prototyp Journal* 24 (2018) 1067–1075, <https://doi.org/10.1108/RPJ-11-2017-0242>.
- [117] V. Mazzanti, L. Malagutti, F. Mollica, FDM 3D printing of polymers containing natural fillers: a review of their mechanical properties, *Polymers (Basel)* 11 (2019) <https://doi.org/10.3390/polym11071094>.
- [118] R. Guo, Z. Ren, H. Bi, Y. Song, M. Xu, Effect of toughening agents on the properties of poplar wood flour/poly (lactic acid) composites fabricated with fused deposition modeling, *Eur. Polym. J.* 107 (2018) 34–45.
- [119] A. Le Duigou, A. Barbé, E. Guillou, M. Castro, 3D printing of continuous flax fibre reinforced biocomposite for structural applications, *Mater. Des.* 180 (2019), 107884, <https://doi.org/10.1016/j.matdes.2019.107884>.
- [120] R. Matsuzaki, M. Ueda, M. Namiki, T.-K. Jeong, H. Asahara, K. Horiguchi, et al., Three-dimensional printing of continuous-fiber composites by in-nozzle impregnation, *Sci. Rep.* 6 (2016), 23058, <https://doi.org/10.1038/srep23058>.
- [121] Y. Dong, J. Milentis, A. Pramanik, Additive manufacturing of mechanical testing samples based on virgin poly (lactic acid) (PLA) and PLA/wood fibre composites, *Adv. Manuf.* 6 (2018) 71–82.
- [122] S. Guessasma, S. Belhabib, H. Nouric, Understanding the microstructural role of bio-sourced 3D printed structures on the tensile performance, *Polym. Test.* (2019) 77.
- [123] Q. Tarrés, J.K. Melbø, M. Delgado-Aguilar, F.X. Espinach, P. Mutjé, G. Chinga-Carrasco, Bio-polyethylene reinforced with thermomechanical pulp fibers: mechanical and micromechanical characterization and its application in 3D-printing by fused deposition modelling, *Compos Part B Eng* 153 (2018) 10–17.
- [124] S. Guessasma, S. Belhabib, H. Nouri, Microstructure and mechanical performance of 3D printed wood-PLA/PHA using fused deposition modelling: effect of printing temperature, *Polymers (Basel)* 11 (2019) <https://doi.org/10.3390/polym11111778>.
- [125] K. Vigneshwaran, N. Venkateshwaran, Statistical analysis of mechanical properties of wood-PLA composites prepared via additive manufacturing, *Int. J. Polym. Anal. Charact.* (2019) <https://doi.org/10.1080/1023666X.2019.1630940>.
- [126] N. Ayrilmis, M. Kariz, J. Kwon, M. Kuzman, Effect of printing layer thickness on water absorption and mechanical properties of 3D-printed wood/PLA composite materials, *Int. J. Adv. Manuf. Technol.* 102 (2019) 2195–2200.
- [127] D. Stoof, K. Pickering, 3D printing of natural fibre reinforced recycled polypropylene, *Process Fabr Adv Mater* (2017) 668–691.
- [128] H.L. Tekinalp, V. Kunc, G.M. Velez-Garcia, C.E. Duty, L.J. Love, A.K. Naskar, et al., Highly oriented carbon fiber-polymer composites via additive manufacturing, *Compos. Sci. Technol.* 105 (2014) 144–150, <https://doi.org/10.1016/j.compscitech.2014.10.009>.
- [129] F. Ning, W. Cong, Y. Hu, H. Wang, Additive manufacturing of carbon fiber-reinforced plastic composites using fused deposition modeling: effects of process parameters on tensile properties, *J. Compos. Mater.* (2017) 51.
- [130] O.S. Carneiro, A.F. Silva, R. Gomes, Fused deposition modeling with polypropylene, *Mater. Des.* 83 (2015) 768–776.
- [131] R. Ferreira, I. Amatte, T. Dutra, D. Burger, Experimental characterization and micrography of 3D printed PLA and PLA reinforced with short carbon fibers, *Compos Part B Eng* (2017) 88–100, <https://doi.org/10.1016/j.compositesb.2017.05.013>.
- [132] F. Van Der Klift, Y. Koga, A. Todoroki, M. Ueda, Y. Hirano, R. Matsuzaki, 3D printing of continuous carbon fibre reinforced thermo-plastic (CFRTP) tensile test specimens, *Open J Compos Mater* 6 (2016) 18–27, <https://doi.org/10.4236/ojcm.2016.61003>.
- [133] A.N. Dickson, J.N. Barry, K.A. McDonnell, D.P. Dowling, Fabrication of continuous carbon, glass and Kevlar fibre reinforced polymer composites using additive manufacturing, *Addit Manuf* 16 (2017) 146–152, <https://doi.org/10.1016/j.addma.2017.06.004>.
- [134] G. Chabaud, M. Castro, C. Denoual, A. Le Duigou, Hygro-mechanical properties of 3D printed continuous carbon and glass fibre reinforced polyamide composite for outdoor structural applications, *Addit Manuf* 26 (2019) 94–105.
- [135] B. Akhondi, A. Behravesh, A. Saed, Improving mechanical properties of continuous fiber-reinforced thermoplastic composites produced by FDM 3D printer, *J. Reinf. Plast. Compos.* (2018) 1–18, <https://doi.org/10.1177/0731684418807300>.
- [136] K. Oksman, M. Skrifvars, J.-F. Selin, Natural fibres as reinforcement in polylactic acid (PLA) composites, *Compos. Sci. Technol.* 63 (2003) 1317–1324, [https://doi.org/10.1016/S0266-3538\(03\)00103-9](https://doi.org/10.1016/S0266-3538(03)00103-9).

- [137] B. Bax, J. Müssig, Impact and tensile properties of PLA/Cordenka and PLA/flax composites, *Compos. Sci. Technol.* 68 (2008) 1601–1607, <https://doi.org/10.1016/j.compscitech.2008.01.004>.
- [138] A. Le Duigou, A. Bourmaud, P. Davies, C. Baley, Long term immersion in natural seawater of Flax/PLA biocomposite, *Ocean Eng.* 90 (2014) 140–148, <https://doi.org/10.1016/j.oceaneng.2014.07.021>.
- [139] E. Bodros, I. Pillin, N. Montrelay, C. Baley, Could biopolymers reinforced by randomly scattered flax fibre be used in structural applications? *Compos. Sci. Technol.* 67 (2007) 462–470, <https://doi.org/10.1016/j.compscitech.2006.08.024>.
- [140] G. Ausias, A. Bourmaud, G. Coroller, C. Baley, Study of the fibre morphology stability in polypropylene-flax composites, *Polym. Degrad. Stab.* 98 (2013) 1216–1224, <https://doi.org/10.1016/j.polymdegradstab.2013.03.006>.
- [141] H. Li, M. Sain, High stiffness natural fiber-reinforced hybrid polypropylene composites, *Polym Plast Technol Eng* 42 (2003) 853–862.
- [142] C. Baley, M. Lan, A. Bourmaud, A. Le Duigou, Compressive and tensile behaviour of unidirectional composites reinforced by natural fibres: influence of fibres (flax and jute), matrix and fibre volume fraction, *Mater Today Commun* (2018) <https://doi.org/10.1016/j.jmtcomm.2018.07.003>.
- [143] A. Bourmaud, A. Le Duigou, C. Gourier, C. Baley, Influence of processing temperature on mechanical performance of unidirectional polyamide 11-flax fibre composites, *Ind. Crop. Prod.* 84 (2016) 151–165, <https://doi.org/10.1016/j.indcrop.2016.02.007>.
- [144] A. Monti, A. El Mahi, Z. Jendli, L. Guillaumat, Mechanical behaviour and damage mechanisms analysis of a flax-fibre reinforced composite by acoustic emission, *Compos Part A Appl Sci Manuf* 90 (2016) 100–110, <https://doi.org/10.1016/j.compositesa.2016.07.002>.
- [145] C. Baley, A. Kervoëlen, M. Lan, D. Cartier, A. Le Duigou, A. Bourmaud, et al., Flax/PP manufacture by automated fibre placement (AFP), *Mater. Des.* (2016) 94.
- [146] S. Liang, P.-B. Gning, L. Guillaumat, Quasi-static behaviour and damage assessment of flax/epoxy composites, *Mater. Des.* 67 (2015) 344–353, <https://doi.org/10.1016/j.matdes.2014.11.048>.
- [147] A. Lefeuvre, A. Bourmaud, C. Baley, Optimization of the mechanical performance of UD flax/epoxy composites by selection of fibres along the stem, *Compos Part A Appl Sci Manuf* 77 (2015) 204–208, <https://doi.org/10.1016/j.compositesa.2015.07.009>.
- [148] T. Cadu, M. Berges, O. Sicot, V. Person, B. Piezel, L. Van Schoors, et al., What are the key parameters to produce a high-grade bio-based composite? Application to flax/epoxy UD laminates produced by thermocompression, *Compos Part B Eng* 150 (2018) 36–46.
- [149] I. Van de Weyenberg, J. Ivens, A. De Coster, B. Kino, E. Baetens, I. Verpoest, Influence of processing and chemical treatment of flax fibres on their composites, *Compos. Sci. Technol.* 63 (2003) 1241–1246, [https://doi.org/10.1016/S0266-3538\(03\)00993-9](https://doi.org/10.1016/S0266-3538(03)00993-9).
- [150] J. Baets, D. Plastria, J. Ivens, I. Verpoest, Determination of the optimal flax fibre preparation for use in unidirectional flax–epoxy composites, *J. Reinf. Plast. Compos.* 33 (2014) 493–502, <https://doi.org/10.1177/0731684413518620>.
- [151] A.R. Torrado, D.A. Roberson, Failure analysis and anisotropy evaluation of 3D-printed tensile test specimens of different geometries and print raster patterns, *J. Fail. Anal. Prev.* 16 (2016) 154–164, <https://doi.org/10.1007/s11668-016-0067-4>.
- [152] L. Pyl, K.-A. Kalteremidou, D. Van Hemelrijck, Exploration of specimens' geometry and tab configuration for tensile testing exploiting the potential of 3D printing freeform shape continuous carbon fibre-reinforced nylon matrix composites, *Polym. Test.* 71 (2018) 318–328.
- [153] M. Fernandez-Vicente, W. Calle, S. Ferrandiz, A. Conejero, Effect of infill parameters on tensile mechanical behavior in desktop 3D printing, *3D Print Addit Manuf* 3 (2016) 183–192, <https://doi.org/10.1089/3dp.2015.0036>.
- [154] G. Goh, V. Dikshit, A. Nagalingam, G. Goh, S. Agarwala, S. Sing, et al., Characterization of mechanical properties and fracture mode of additively manufactured carbon fiber and glass fiber reinforced thermoplastics, *Mater. Des.* 137 (2018) 79–89.
- [155] J. Baets, D. Plastria, J. Ivens, I. Verpoest, Determination of the optimal flax fibre preparation for use in unidirectional flax–epoxy composites, *J. Reinf. Plast. Compos.* 33 (2014) 493–502.
- [156] N. Sanandiyaya, Y. Vijay, M. Dimopoulou, S. Dritsas, J. Fernandez, Large-scale additive manufacturing with bioinspired cellulose materials, *Sci Reports* 8 (2018) 8642.
- [157] J. Zhou, S. Sheiko, Reversible shape-shifting in polymeric materials, *J Polym Sci Part B Polym Phys* 54 (2016) 1365–1380, <https://doi.org/10.1002/polb.24014>.
- [158] L. Sun, W. Huang, Mechanisms of the multi-shape memory effect and temperature memory effect in shape memory polymers, *Soft Matter* 6 (2010) 4403, <https://doi.org/10.1039/c0sm00236d>.
- [159] L. Sun, W.M. Huang, Z. Ding, Y. Zhao, C.C. Wang, H. Purnawali, et al., Stimulus-responsive shape memory materials: a review, *Mater. Des.* 33 (2012) 577–640, <https://doi.org/10.1016/j.matdes.2011.04.065>.
- [160] M.C. Mulakkal, R.S. Trask, V.P. Ting, A.M. Seddon, Responsive cellulose-hydrogel composite ink for 4D printing, *Mater. Des.* 160 (2018) 108–118, <https://doi.org/10.1016/j.matdes.2018.09.009>.
- [161] A. Baker, S. Bates, T. Llewellyn-Jones, L. Valori, M. Dicker, R. Trask, 4D printing with robust thermoplastic polyurethane hydrogel-elastomer trilayers, *Mater. Des.* 167 (2019), 107544, <https://doi.org/10.1016/j.matdes.2018.107544>.
- [162] C. Yuan, T. Wang, M. Dunn, H. Qi, 3D printed active origami with complicated folding patterns, *Int J Precis Eng Manuf-Gr Technol* 4 (2017) 281–289.
- [163] Q. Ge, C. Dunn, H. Qi, M. Dunn, Active origami by 4D printing, *Smart Mater. Struct.* 23 (2014) 15.
- [164] M. Bodaghi, A. Damanpack, W. Liao, Self-expanding/shrinking structures by 4D printing, *Smart Mater. Struct.* 25 (2016) 15.
- [165] D. Kokkinis, M. Schaffner, A. Studart, Multimaterial magnetically assisted 3D printing of composite materials, *Nat. Commun.* 6 (2015) 8643.
- [166] C. Yang, B. Wang, D. Li, X. Tian, Modelling and characterisation for the responsive performance of CF/PLA and CF/PEEK smart materials fabricated by 4D printing, *Virtual Phys Prototyp* 12 (2017) 69–76.
- [167] R. Stahlberg, M. Taya, What can we learn from nastic plant structures? The phytomimetic potentiality of nastic structures, *Proc. SPIE* 6168 (2006) <https://doi.org/10.1117/12.658924> Smart Stru.
- [168] A. Le Duigou, M. Castro, Evaluation of force generation mechanisms in natural, passive hydraulic actuators, *Sci. Rep.* 6 (2016) 1–9 18105.
- [169] I. Burgert, P. Fratzl, Actuation systems in plants as prototypes for bioinspired devices, *Philos. Trans. R. Soc. A Math. Phys. Eng. Sci.* 367 (2009) 1541–1557.
- [170] R. Elbaum, Y. Abraham, Insights into the microstructures of hygroscopic movement in plant seed dispersal, *Plant Sci.* 223 (2014) 124–133, <https://doi.org/10.1016/j.plantsci.2014.03.014>.
- [171] J.W.C. Dunlop, R. Weinkamer, P. Fratzl, Artful interfaces within biological materials, *Mater. Today* 14 (2011) 70–78, [https://doi.org/10.1016/S1369-7021\(11\)70056-6](https://doi.org/10.1016/S1369-7021(11)70056-6).
- [172] M. Rüggeberg, I. Burgert, Bio-inspired wooden actuators for large scale applications, *PLoS One* 10 (2015), e0120718, <https://doi.org/10.1371/journal.pone.0120718>.
- [173] S. Reichert, A. Menges, D. Correa, Meteorosensitive architecture: biomimetic building skins based on materially embedded and hygroscopically enabled responsiveness, *Comput. Des.* 60 (2015) 50–69, <https://doi.org/10.1016/j.cad.2014.02.010>.
- [174] G. Holstov, G. Farmer, B. Bridgens, Sustainable materialisation of responsive architecture, *Sustainability* 9 (2017) 1–20.
- [175] C. Vailati, E. Bachtari, P. Hass, M.R. Burgert I, An autonomous shading system based on coupled wood bilayer elements, *Energy Build* 158 (2017) 1013–1022.
- [176] L. Guiducci, K. Razghandi, L. Bertinetti, S. Turcaud, M. Rüggeberg, J.C. Weaver, et al., Honeycomb actuators inspired by the unfolding of ice plant seed capsules, *PLoS One* 11 (2016) 1–21.
- [177] Y. Lining, O. Jifei, W. Guanyun, C. Chin-Yi, W. Wen, S. Helene, I. Hiroshi, Bio print: a liquid deposition printing system for natural actuators, *3D Print Addit Manuf* 2 (2015) 168–179.
- [178] X. Chen, L. Mahadevan, A. Driks, O. Sahin, Bacillus spores as a building blocks for stimuli-responsive materials and nanogenerators, *Nat Nanotechnol Lett* 9 (2014) 137–141.
- [179] Q. Wang, X. Tian, L. Huang, D. Li, A.V. Malakhov, A.N. Polilov, Programmable morphing composites with embedded continuous fibers by 4D printing, *Mater. Des.* 155 (2018) 404–413.
- [180] A. Rayate, P. Jain, A review on 4D printing material composites and their applications, *Mater Today Commun* 5 (2018).
- [181] S. Turcaud, L. Guiducci, P. Fratzl, Y. Brechet, J. Dunlop, An excursion into the design space of biomimetic architected biphasic actuator, *Int. J. Mater. Res.* (2011) 102.
- [182] E. Reysat, L. Mahadevan, Hygromorph: from pine cone to biomimetic bilayers, *J R Soc* 6 (2009) 951–957.
- [183] D. Correa, A. Papadopoulou, C. Guberan, N. Jhaveri, S. Reichert, A. Menges, et al., 3D printing wood: programming hygroscopic material transformations, *3D Print Addit Manuf* 2 (2015) 106–116.
- [184] E. Vazquez, B. Gursoy, J. Duarte, Designing for Shape Change: A Case Study on 3D Printing Composite Materials for Responsive Architectures. Conference, 2019 391–400.
- [185] P. Zhang, P. Chen, B. Wang, R. Yu, H. Pan, B. Wang, Evaluating the hierarchical, hygroscopic deformation of the Daucus carota umbel through structural characterization and mechanical analysis, *Acta Biomater.* 99 (2019) 457–468.
- [186] D. Van Opdenbosch, G. Fritz-Popovski, W. Wagermaier, O. Paris, C. Zollfrank, Moisture-driven ceramic bilayer actuators from a biotemplating approach, *Adv. Mater.* 28 (2016) 5235–5240.
- [187] Q. Zhao, J. Dunlop, X. Qiu, F. Huang, Z. Zhang, J. Heyda, et al., An instant multi-responsive porous polymer actuator driven by solvent molecule sorption, *Nat. Commun.* 5 (2014).
- [188] C. Vailati, P. Hass, I. Burgert, M. Rüggeberg, Upscaling of wood bilayers: design principles for controlling shape change and increasing moisture change rate, *Mater. Struct.* 50 (2017) <https://doi.org/10.1617/s11527-017-1117-4>.
- [189] E. Vazquez, B. Gursoy, J. Duarte, Formalizing shape-change: three-dimensional printed shapes and hygroscopic material transformations, *Int. J. Archit. Comput.* (2019) 1–17, <https://doi.org/10.1177/1478077119895216>.
- [190] D. Correa, S. Poppinga, M. Mylo, A. Westermeier, B. Bruchmann, A. Menges, et al., 4D pine scale: biomimetic 4D printed autonomous scale and flap structures capable of multi-phase movement, *Philos Trans A Math Phys Eng Sci* 378 (2020), 20190445, <https://doi.org/10.1098/rsta.2019.0445>.
- [191] A. Holstov, B. Bridgens, G. Farmer, Hygromorphic materials for sustainable responsive architecture, *Constr. Build. Mater.* 98 (2015) 570–582, <https://doi.org/10.1016/j.conbuildmat.2015.08.136>.
- [192] S. Lin, Y. Xie, Q. Lib, X. Huang, S. Zhou, On the shape transformation of cone scales, *Soft Matter* 12 (2016) 9797–9802.
- [193] S. Poppinga, T. Speck, New insight into the passive motions of pine cone and false indusia in ferns, *Plant Biomech* 8 (2015).
- [194] Y. Liu, J. Genzer, M. Dickey, 2D or not 2D: shape programming polymer sheets, *Prog. Polym. Sci.* 52 (2016) 79–106.
- [195] A. Le Duigou, V. Keryvin, J. Beaugrand, M. Pernes, F. Scarpa, M. Castro, Humidity responsive actuation of bioinspired hygromorph biocomposites (HBC) for adaptive structures, *Compos. Part A* 116 (2019) 36–45, <https://doi.org/10.1016/j.compositesa.2018.10.018>.
- [196] C. Vailati, M. Rüggeberg, I. Burgert, P. Hass, The kinetics of wooden bilayers is not affected by different wood adhesive systems, *Wood Sci. Technol.* 52 (2018) <https://doi.org/10.1007/s00226-018-1046-6>.

- [197] D. Wood, C. Vailati, A. Menges, M. Rüggeberg, Hygroscopically actuated wood elements for weather responsive and self-forming building parts – facilitating upscaling and complex shape changes, *Constr. Build. Mater.* 165 (2018) 782–791.
- [198] 4D Printing Market, By application (aerospace and defense, healthcare, automotive, construction, clothing, utility, others.), by region-global forecast to 2022, *Mark Res Futur* (2020) , ID: MRFR/S. doi <https://www.marketresearchfuture.com/reports/4d-printing-market-2692> 100 pages.
- [199] F. Sullivan, *And. Advances in 4D Printing—Next Paradigm in Manufacturing*, Rep D545-TI, 2014.
- [200] S. Tibbits, 4D printing: multi-material shape change, *Archit. Des.* (2014) 116–121.
- [201] M.F. Pucci, P.-J. Liotier, S. Drapier, Capillary wicking in flax fabrics – effects of swelling in water, *Colloids Surfaces A Physicochem Eng Asp* 498 (2016) 176–184, <https://doi.org/10.1016/j.colsurfa.2016.03.050>.
- [202] M. Deroiné, A. Le Duigou, Y.-M. Corre, P.-Y. Le Gac, P. Davies, G. César, et al., Accelerated ageing of polylactide in aqueous environments: comparative study between distilled water and seawater, *Polym. Degrad. Stab.* (2014) <https://doi.org/10.1016/j.polydegradstab.2014.01.020>.
- [203] A. Le Duigou, G. Chabaud, F. Scarpa, M. Castro, Bioinspired electro-thermo-hygro-reversible shape changing materials by 4D printing, *Adv. Funct. Mater.* (2019), 1903280. <https://doi.org/10.1002/adfm.201903280>.
- [204] R. Lincoln, F. Scarpa, V. Ting, R. Trask, Multifunctional composites: a metamaterial perspective, *Multifunc Mater* (2019) <https://doi.org/10.1088/2399-7532/ab5242>.
- [205] S. Poppinga, D. Correa, B. Bruchmann, A. Menges, T. Speck, Plant movements as concept generators for the development of biomimetic compliant mechanisms, *Integr. Comp. Biol.* (2020) <https://doi.org/10.1093/icb/icaa028>.
- [206] S. Turcaud, Some patterns of shape change controlled by eigenstrain architectures, Thesis Report <https://tel.archives-ouvertes.fr/tel-01206053> 2015.
- [207] L. Guiducci, Weaver, Y. Bréchet, P. Fratzl, J. Dunlop, The geometric design and fabrication of actuating cellular structures, *Adv. Mater. Interfaces* 2 (2015), 1500011..